

FILE COPY  
NO. 1-W

# CASE FILE COPY

ARR No. 3K17

NATIONAL ADVISORY COMMITTEE FOR AERONAUTICS

# WARTIME REPORT

ORIGINALLY ISSUED

November 1943 as  
Advance Restricted Report 3K17

THEORETICAL ANALYSIS OF THE LATERAL STABILITY

OF A GLIDER TOWED BY TWIN PARALLEL TOWLINES

By Marvin Pitkin and Marion O. McKinney, Jr.

Langley Memorial Aeronautical Laboratory  
Langley Field, Va.

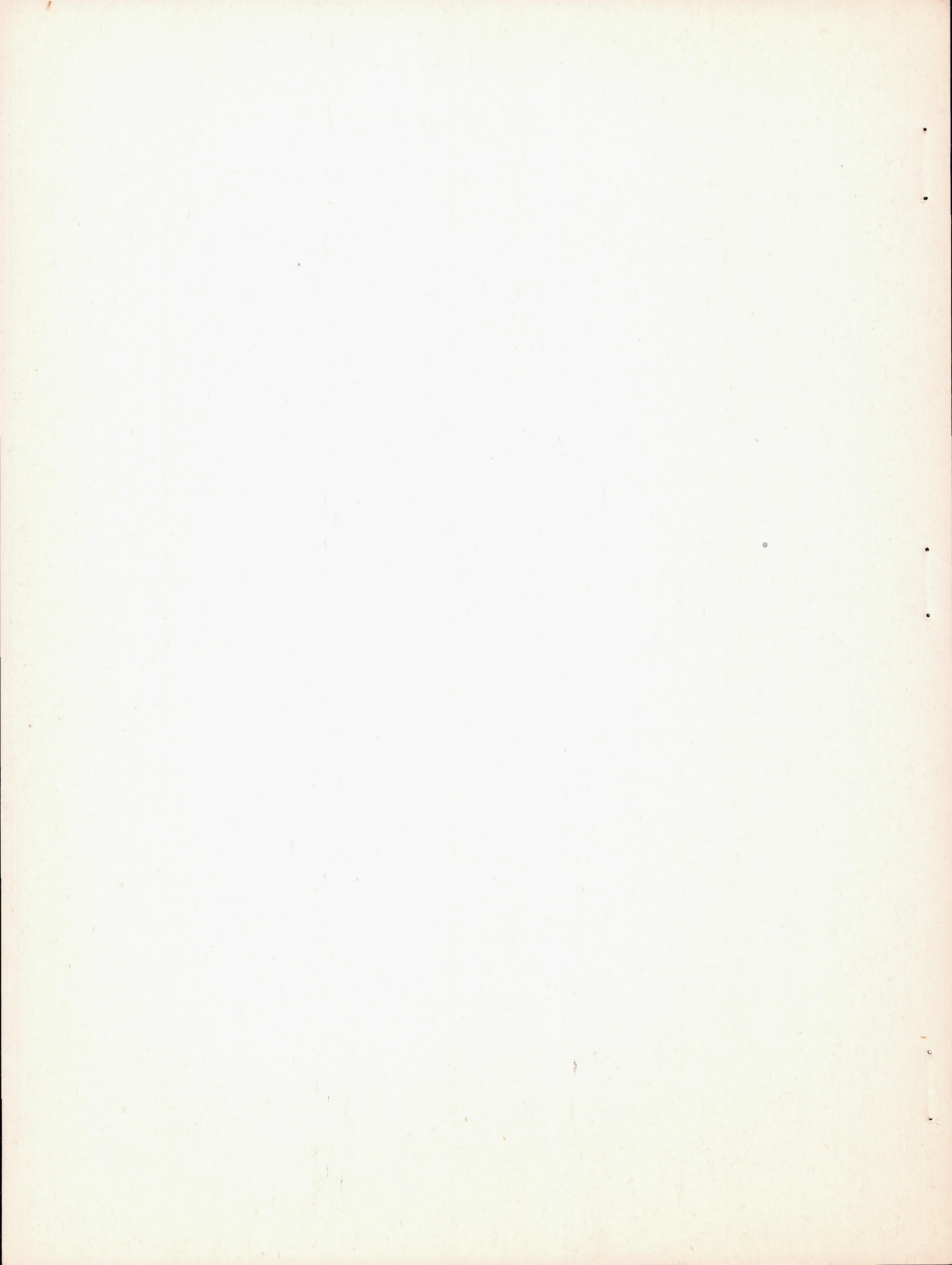
**FILE COPY**

To be returned to  
the files of the National  
Advisory Committee  
for Aeronautics  
Washington D. C.



WASHINGTON

NACA WARTIME REPORTS are reprints of papers originally issued to provide rapid distribution of advance research results to an authorized group requiring them for the war effort. They were previously held under a security status but are now unclassified. Some of these reports were not technically edited. All have been reproduced without change in order to expedite general distribution.



NATIONAL ADVISORY COMMITTEE FOR AERONAUTICS

ADVANCE RESTRICTED REPORT

THEORETICAL ANALYSIS OF THE LATERAL STABILITY  
OF A GLIDER TOWED BY TWIN PARALLEL TOWLINES

By Marvin Pitkin and Marion O. McKinney, Jr.

SUMMARY

A theoretical analysis of the lateral stability characteristics of a glider towed by two parallel towlines has been made and correlated with previously reported dynamic flight tests of a glider model in the NACA free-flight tunnel. Calculations were made for a range of effective dihedral angles from  $-6^{\circ}$  to  $14^{\circ}$ , a range of towline lengths from one to three glider spans, lift coefficients of 0.30 and 0.75, and a range of glider lift-drag ratios from 4.5 to 21.0. The results of the theoretical analysis indicated that a glider towed by twin parallel cables possesses sufficient stability for satisfactory pilotless towed flight.

The stability of the glider was found to be primarily dependent upon the dihedral angle of the glider and the length of the towlines. Both unstable oscillations and divergences were found to occur either at negative or at large positive effective dihedral angles. A maximum of stability was indicated at moderate positive dihedral angles. The stability of the glider was decreased as the towline length and lift coefficient increased. Large sidewise displacements of the glider relative to the tug reduced the stability, particularly when the dihedral angle was large. Agreement between theoretical and flight results was very satisfactory.

INTRODUCTION

Load-carrying gliders may be used to carry troops or cargo to supplement the carrying capacity of existing airplanes without seriously decreasing the efficiency of the tug. In order to realize full benefit from such an arrangement it is desirable to have inherent stability in

the glider system. An adequate degree of stability would eliminate the need for a pilot in the glider or would at least relieve the pilot of the necessity of giving constant attention to the controls. Although some success has been obtained with a single towline glider system, considerable difficulty has been experienced in obtaining a sufficient degree of lateral stability. A somewhat simpler system for securing stability appears to be one involving twin parallel towlines attached near the wing tips of the glider to restrain the glider from yawing. A preliminary investigation (reference 1) in the NACA free-flight tunnel indicated that a stable pilotless towed glider system was possible with twin parallel towlines.

In order to obtain an understanding of the operation of this yawing restraint in providing lateral stability and to allow an extension of the results to other glider configurations, a theoretical analysis has been made of the lateral stability of the system. Calculations were made for the Bristol tow-target glider "Skeet" to correlate the theory with the tests of reference 1.

#### SYMBOLS

W	weight of the glider, pounds
m	mass of the glider, slugs
b	span of the glider, feet
$b_1$	distance along Y-axis from the center of gravity of the glider to the towline attachment points, feet
S	wing area of the glider, square feet
X, Y, Z	centroidal axes of glider
a	length of the towlines, feet
$a'$	length of towlines in glider span lengths ( $a/b$ )
$k_x$	radius of gyration about the X axis, feet
A', B', C'	space axes parallel to the body axes of the tug intersecting midway between the towline attachment points on the tug

L-572

$\epsilon$	angle between towline and A'-axis, radians
$V$	true airspeed, feet per second
$\beta$	angle of sideslip, radians
$y$	sidewise displacement of glider center of gravity along the B'-axis, feet
$y'$	sidewise displacement in glider span lengths $(y/b)$
$v$	sideslip velocity, feet per second
$\phi$	angle of bank, radians
$p$	rolling angular velocity, radians per second
$\psi$	angle of yaw, degrees
$D$	drag of glider, pounds; differential operator $\left(\frac{d}{ds}\right)$
$T$	towline tension, pounds
$C_L$	lift coefficient $\left(\frac{\text{lift}}{\frac{\rho}{2}SV^2}\right)$
$C_D$	drag coefficient $\left(\frac{\text{drag}}{\frac{\rho}{2}SV^2}\right)$
$\rho$	density of air, slugs per cubic foot
$t$	time, seconds
$\mu$	airplane relative-density factor $(m/\rho S b)$
$L$	rolling moment of glider, foot-pounds
$Y$	lateral force of glider, pounds
$C_l$	rolling-moment coefficient $\left(\frac{L}{\frac{\rho}{2}SV^2 b}\right)$
$C_y$	lateral-force coefficient $\left(\frac{Y}{\frac{\rho}{2}SV^2}\right)$

$Y_v$	rate of change of lateral force with sidewise velocity $(\partial Y/\partial v)$
$Y_\psi$	rate of change of lateral force with angle of yaw $(\partial Y/\partial \psi)$
$(Y_y)_1$	rate of change of lateral force induced by towline tension with glider sidewise displacement $(\partial Y/\partial y)_1$
$(Y_\phi)_2$	rate of change of lateral force due to yaw produced by sideslip and roll with angle of roll $(\partial Y/\partial \phi)_2$
$L_p$	rate of change of rolling moment with rolling velocity $(\partial L/\partial p)$
$L_v$	rate of change of rolling moment with sideslip velocity $(\partial L/\partial v)$
$L_\psi$	rate of change of rolling moment with angle of yaw $(\partial L/\partial \psi)$
$(L_\phi)_1$	rate of change of rolling moment induced by towline tension with angle of roll $(\partial L/\partial \phi)_1$
$(L_\phi)_2$	rate of change of rolling moment due to yaw produced by sideslip and roll with angle of roll $(\partial L/\partial \phi)_2$
$(\overline{L_\phi})_2$	effective rate of change of rolling moment due to yaw produced by sideslip and roll with angle of roll $\left(\frac{\partial \overline{L}}{\partial \phi}\right)_2$
$(\overline{Y_\phi})_2$	effective rate of change of lateral force due to yaw produced by sideslip and roll with angle of roll $\left(\frac{\partial \overline{Y}}{\partial \phi}\right)_2$
$(C_{Y\beta})$	rate of change of lateral-force coefficient with angle of sideslip, per radian $(\partial C_Y/\partial \beta)$
$(C_{Y_y})_1$	rate of change of lateral-force coefficient induced by towline tension with sidewise displacement $(\partial C_Y/\partial y')_1$

$(\overline{C_{Y\phi}})_2$	effective rate of change of lateral-force coefficient due to angle of yaw produced by sideslip and roll with angle of roll
$\left(\frac{\partial \overline{C_Y}}{\partial \phi}\right)_2$	
$C_{l\beta}$	rate of change of rolling-moment coefficient with angle of sideslip, per radian $(\partial C_l / \partial \beta)$
$C_{lp}$	rate of change of rolling-moment coefficient with helix angle $\left(\partial C_l / \partial \frac{pb}{2V}\right)$
$(C_{l\phi})_1$	rate of change of rolling-moment coefficient induced by towline tension with angle of roll $(\partial C_l / \partial \phi)_1$
$(\overline{C_{l\phi}})_2$	effective rate of change of rolling-moment coefficient due to angle of yaw produced by sideslip and roll with angle of roll $\left(\frac{\partial \overline{C_l}}{\partial \phi}\right)_2$
s	forward distance traveled in span lengths $\left(\frac{v}{b}t\right)$
$\lambda$	root of the stability quartic
A, B, C, E, F	coefficients of the stability quartic
R	Routh's discriminant $(BCE - E^2 - B^2F)$
id	imaginary portion of a complex root
c	real portion of a complex root or a real root
P	period of oscillation, seconds
$t_{1/2}$	time required for motion to damp to one-half amplitude, seconds
$\Gamma$	geometric dihedral angle, degrees
$\Gamma_{\text{eff}}$	effective dihedral angle, degrees $(-C_{l\beta} / 0.012)$

L-572

## METHODS

The analysis of the lateral stability of a glider attached to a towing airplane by twin parallel towlines was made by setting up the stability equations, obtaining the stability derivatives when necessary, and then calculating the stability boundaries, the period of the oscillatory (periodic) mode, and the damping of the oscillatory and the aperiodic components of the glider motion.

## Assumptions

In order to facilitate the handling of the theoretical investigation the following assumptions were made:

(1) Level tow: The tug and glider were assumed to be in level flight with the towlines horizontal.

(2) Straight towlines: The towlines were assumed weightless and straight. This assumption is justified by the flight data of the investigation reported in reference 1. Thus, no derivatives considering the weight and curvature were included.

(3) Two degrees of lateral freedom: The glider was considered to be restricted by the towlines to two degrees of lateral freedom.

(4) Towpoint attachments on Y-axis: The glider was assumed to be attached at two points on the Y-axis.

## Equations of Motion

Inasmuch as the dyadic towline system restrains the glider from yawing, only two degrees of lateral freedom need be considered in setting up the equations of motion that apply to this problem. The lateral-force and rolling-moment equations after a disturbance may consequently be written as

$$m \frac{dy}{dt} = W\phi + v \frac{\partial Y}{\partial v} + \text{towline derivatives} \quad (1)$$

$$mk_X \frac{dp}{dt} = p \frac{\partial L}{\partial p} + v \frac{\partial L}{\partial v} + \text{towline derivatives} \quad (2)$$



The problem therefore becomes one of evaluating the towline derivatives. When this step is accomplished, the stability equations may be set up and treated mathematically to obtain definition of glider stability.

L-572

### Towline Derivatives

Derivatives due to cable tension.- Two towline derivatives due to cable tension may be obtained from inspection of figure 1. A sidewise displacement of the glider along the direction of its Y-axis is opposed by a component of cable tension. The derivative expressing the resultant relationship is then

$$\begin{aligned} (Y_y)_1 &= \left( \frac{\partial Y}{\partial y} \right)_1 \\ &= \frac{-\text{Tension (or drag)}}{\text{Towline length}} \\ &= \frac{-D}{a} \end{aligned} \quad (3)$$

Similarly, the towline tension resists the effort of the glider to assume a banked attitude. The derivative defining this relationship is

$$\begin{aligned} (L_\phi)_1 &= \left( \frac{\partial L}{\partial \phi} \right)_1 \\ &= \frac{\text{Tension (or drag)} \times b_1^2}{\text{Towline length}} \\ &= \frac{-Db_1^2}{a} \end{aligned} \quad (4)$$

The nondimensional form of these equations is

$$(C_{Y_y'})_1 = \frac{-C_D}{a'} \quad (5)$$

and

$$(C_{L_\phi})_1 = \frac{-C_D}{a'} \left( \frac{b_1}{b} \right)^2 \quad (6)$$

The towline derivatives  $(C_{\dot{\nu}\phi})_1$  and  $(C_{\dot{\gamma}y'})_1$  are the only first-order terms contributed by the towlines. Inasmuch as conventional stability theory assumes that only first-order terms are considered, these terms were the only towline derivatives to be introduced into the equations of motion (1) and (2) in the early phases of the investigation. The glider stability was then calculated.

The results of these initial calculations were somewhat in disagreement with the model flight data of reference 1 because the calculations did not predict instability at the large dihedral angles at which unstable oscillations had been encountered in the flight tests. A clue to the correct solution was obtained from a further analysis of data previously obtained from flights of the model with large dihedral angles. The model was observed to fly satisfactorily during the tests of reference 1 provided that the tunnel air-flow disturbances were small. For large disturbances involving large glider displacements, however, the model quickly developed an unstable oscillation. This phenomenon indicated that large displacements were introducing unstable effects sufficiently large to overcome the inherent stability of the glider system for small oscillations. It thus appeared likely that some second-order effect existed which was sufficiently large at large values of glider displacement to induce instability.

An analysis was therefore made in an effort to determine which, if any, of the second-order terms of the glider system could have an appreciable effect upon glider stability. This analysis indicated that the second-order effects of the derivatives hitherto discussed would be of small magnitude, even for large values of glider displacement. It was observed, however, that new towline derivatives, second-order in form, arose from glider displacement and were of sufficient magnitude for large displacements to induce instability. These derivatives resulted from the geometric characteristics of the parallelogram formed by the towlines and the tug and glider wing spans. The derivation of these derivatives and the method of introducing them into the glider equations is discussed in the following section.

Second-order derivatives due to glider position.— The geometric characteristics of the parallelogram formed by

L-372

the towlines and the tug and glider wings are such that, if the glider sideslips and robs relative to the tug, the towlines force the glider into a yawed attitude. In horizontal tow this action results in positive yaw accompanying positive sidewise displacement. This angle of yaw introduces additional stability derivatives that are dependent upon the amount of sidewise displacement and bank. If the effects of yawing velocity, which are believed to be small, are neglected, the rolling moment  $L$  and the lateral force  $Y$  due to the angle of yaw induced by glider position are found to be

$$L = \psi L_{\psi}$$

$$Y = \psi Y_{\psi}$$

But

$$\psi = f(\phi, y)$$

therefore,

$$L = f(\phi, y) L_{\psi} \tag{7}$$

Likewise,

$$Y = f(\phi, y) Y_{\psi} \tag{8}$$

The exact solution for  $\psi$  in terms of  $\phi$  and  $y$  leads to a highly complex equation. An approximate formula, however, has been obtained by spherical trigonometry and checked by means of a mechanical device reproducing the glider tow system. The equation for angle of yaw is

$$\psi = \frac{\phi^2 \tan \epsilon}{1.8 - 0.07(a' - 1)} \tag{9}$$

where

$$\tan \epsilon = \frac{y'}{\sqrt{a'^2 - y'^2}}$$

It should be observed that the sidewise displacement  $y'$  can never exceed the length of the towlines  $a'$ .

The agreement between values of  $\psi$  calculated by means of this equation and the measured values is shown in figure 2, which presents sample values for 1-span towlines. The agreement is equally good for 2- and 3-span towlines.

Substitution of equation (9) in equations (7) and (8) gives the relationships,

$$L = \frac{\phi^2 y' L_{\psi}}{\sqrt{(a')^2 - (y')^2} [1.8 - 0.07(a' - 1)]} \quad (10)$$

and

$$Y = \frac{\phi^2 (y') Y_{\psi}}{\sqrt{(a')^2 - (y')^2} [1.8 - 0.07(a' - 1)]} \quad (11)$$

Steps must now be taken to obtain a relationship between angle of bank  $\phi$  and the sidewise displacement of the glider  $y'$  because, first, an infinite number of solutions for glider stability would otherwise exist and second, insertion of derivatives as a function of  $\phi$  and  $y'$  in the equations of motion would make these differential equations nonlinear and hence unsolvable by conventional mathematical methods.

Although the exact relation of the angle of bank to the sidewise displacement can be found only by a complete solution of the equations of motion, a satisfactory first approximation may be made if the towline and inertia forces are ignored. The relationship of  $\phi$  to  $y'$  may then be expressed by the equation

$$\beta C_{l_{\beta}} + \frac{pb}{2V} C_{l_p} = 0$$

or

$$\beta C_{l_{\beta}} = -\frac{pb}{2V} C_{l_p} \quad (12)$$

The value of  $C_{l_p}$  as used herein has been taken from reference 2 as  $-0.4$ ; then

$$\beta C_{l\beta} = -\frac{pb}{2V} (-0.4)$$

or

$$\frac{y}{V} C_{l\beta} = \frac{pb}{V} (0.2)$$

Multiplying by  $V$  and integrating both sides of this equation with respect to time yields

$$y C_{l\beta} = \phi b (0.2)$$

or

$$\frac{y/b}{\phi} C_{l\beta} = 0.2$$

$$\frac{y'}{\phi} C_{l\beta} = 0.2 \quad (13)$$

The validity of this equation was checked by means of measurements of values of  $y'/\phi$  obtained from motion-picture records of flight tests for various effective dihedral angles and lift coefficients. The test points shown in figure 3 are averages of at least seven readings for each condition and are in satisfactory agreement with calculated results.

Two towline derivatives due to position may now be expressed as a function of either  $\phi$  or  $y'$ . The calculations in this report have utilized values derived as a function of  $\phi$ .

The rolling moment resulting from glider position may be expressed as

$$L = \psi L_{\psi}$$

or, in nondimensional form, as

$$\begin{aligned} C_l &= -\psi C_{l\beta} \\ &= -f(\phi) C_{l\beta} \end{aligned} \quad (14)$$

likewise,

$$\begin{aligned} C_Y &= -\psi C_{Y\beta} \\ &= -f(\phi) C_{Y\beta} \end{aligned} \quad (15)$$

In order to introduce the moments and forces arising from glider position into nondimensional equations of motion, it is convenient to use the relations

$$\begin{aligned} C_l &= \phi \left( \frac{\partial C_l}{\partial \phi} \right)_\alpha \\ &= \phi \left( C_{l\phi} \right)_\alpha \end{aligned} \quad (16)$$

$$\begin{aligned} C_Y &= \phi \left( \frac{\partial C_Y}{\partial \phi} \right)_\alpha \\ &= \phi \left( C_{Y\phi} \right)_\alpha \end{aligned} \quad (17)$$

It is then necessary to evaluate  $\left( C_{l\phi} \right)_\alpha$  and  $\left( C_{Y\phi} \right)_\alpha$ . Inasmuch as  $C_l$  is not a linear function of  $\phi$ ,  $\left( C_{l\phi} \right)_\alpha$  will vary with  $\phi$ . In order to obtain an effective value of  $\left( C_{l\phi} \right)_\alpha$  over any range of values of  $\phi$  from an initial value of  $\phi_0$  to a final value of  $\phi$ , the nonlinear variation of  $C_l$  with  $\phi$  can be replaced by a linear variation which represents the work done in any cycle. This linear variation, effective  $\left( C_{l\phi} \right)_\alpha$ , is derived as follows:

$$\begin{aligned} \text{Work done in } \frac{1}{4} \text{ cycle} &= \left( \frac{\int_{\phi_0}^{\phi} C_l d\phi}{\phi - \phi_0} \right) (\phi - \phi_0) \\ &= \text{mean } \overline{C_l} \Big|_0^{\phi} (\phi - \phi_0) \end{aligned} \quad (18)$$

When  $\Phi_0$  equals 0,

$$\text{Work done in } \frac{1}{4} \text{ cycle} = \overline{C_l} \Phi$$

The linear variation of  $C_l$  with  $\Phi$  yielding the same work in  $\frac{1}{4}$  cycle is consequently defined as

$$\begin{aligned} \text{Effective } \left( C_l \Phi \right)_2 &= \left( \overline{C_l \Phi} \right)_2 \\ &= \frac{2 \overline{C_l} \Phi}{\Phi} \\ &= \frac{2 \int_0^\Phi C_l d\Phi}{\Phi^2} \end{aligned} \quad (19)$$

From equation (14)

$$C_l = -\psi C_{l\beta}$$

Therefore,

$$\left( \overline{C_l \Phi} \right)_2 = -\frac{2 C_{l\beta}}{\Phi^2} \int_0^\Phi \psi d\Phi \quad (20)$$

where, from equation (9),

$$\psi = \frac{\Phi^2}{1.8 - 0.07(a' - 1)} \frac{y'}{\sqrt{a'^2 - y'^2}}$$

and, from equation (13),

$$\Phi = 5 C_{l\beta} y'$$

The integral in equation (20) may be solved in terms of  $\Phi$  or, by rearranging limits, in terms of  $y'$ ; either process yields identical numerical results. Values of  $\left( \overline{C_l \Phi} \right)_2$  are expressed herein as a function of  $y'$ .

Solution of equation (20) in terms of  $y'$  yields, when  $C_{l\beta}$  is negative,

$$\left(\overline{C_{l\phi}}\right)_2 = -\frac{3.33C_{l\beta}^2}{[1.8 - 0.07(a' - 1)] y'^2} \left[ \sqrt{a'^2 - y'^2} (y'^2 + 2a'^2) - 2a'^3 \right] \quad (21)$$

When  $C_{l\beta}$  is positive, the equation is of opposite sign.

The effective derivative  $\left(\overline{C_{Y\phi}}\right)_2$  may be obtained in a similar manner or by the relationship

$$\left(\overline{C_{Y\phi}}\right)_2 = \left(\overline{C_{l\phi}}\right)_2 \frac{C_{Y\beta}}{C_{l\beta}} \quad (22)$$

These towline derivatives are of second order and are dependent upon glider position. The glider stability must therefore be calculated for each sidewise glider position assumed.

The towline derivative  $\left(\overline{C_{l\phi}}\right)_2$  has been plotted against sidewise displacement for various values of  $C_{l\beta}$  and is presented in figure 4 for 1-, 2-, and 3-span towlines.

#### Stability Equations

Substituting the towline derivatives in equations (1) and (2) and rearranging terms yields the following equations:

$$m \frac{dv}{dt} - W\phi - vY_v - y(Y_y)_1 - \phi(\overline{Y_\phi})_2 = 0 \quad (23)$$

$$mk_X \frac{d\phi}{dt} - pL_p - vL_v - \phi(L_\phi)_1 - \phi(\overline{L_\phi})_2 = 0 \quad (24)$$

If the aerodynamic data in standard nondimensional form is to be used and if the original physical signifi-



cance of the equations is to be maintained, a consistent nondimensional system is desirable. The following units for such a nondimensional system were considered convenient:

Unit of length . . . . . b  
 Unit of mass . . . . .  $\rho S b$   
 Unit of time . . . . .  $b/V$

If length, mass, and time are expressed in the nondimensional form, the following nondimensional quantities will result:

$$\mu = \frac{m}{\rho S b}$$

$$s = \frac{V}{b} t$$

Division of the force equation (23) by  $\frac{\rho}{2} S V^2$  and the moment equation (24) by  $\frac{\rho}{2} S V^2 b$  yields the nondimensional equations

$$2\mu D^2 \beta - 2 \frac{\rho b}{2V} \left[ C_L + \left( C_{Y\phi} \right)_2 \right] - D \beta C_{Y\beta} - \beta \left( C_{Y\dot{y}} \right)_1 = 0 \quad (25)$$

$$4\mu \left( \frac{k_X}{b} \right)^2 D^2 \frac{\rho b}{2V} - D \frac{\rho b}{2V} C_{l_p} - D \beta C_{l\beta} - 2 \frac{\rho b}{2V} \left[ \left( C_{l\phi} \right)_1 + \left( C_{l\phi} \right)_2 \right] = 0 \quad (26)$$

The determinant of the left side of these equations yields the glider stability equation of the form

$$A\lambda^4 + B\lambda^3 + C\lambda^2 + E\lambda + F = 0 \quad (27)$$

where

$$A = 1$$

$$B = \frac{1}{8\mu^2 \left( \frac{k_X}{b} \right)^2} \left[ -4\mu \left( \frac{k_X}{b} \right)^2 C_{Y\beta} - 2\mu C_{l_p} \right]$$

$$C * \frac{1}{8\mu^2 \left(\frac{k_X}{b}\right)^2} \left\{ -4\mu \left(\frac{k_X}{b}\right)^2 (C_{Yy'})_1 + C_{Lp} C_{Y\beta} - 4\mu \left[ (C_{l\phi})_1 + (\overline{C_{l\phi}})_2 \right] \right\}$$

$$E = \frac{1}{8\mu^2 \left(\frac{k_X}{b}\right)^2} \left[ (C_{Yy'})_1 C_{Lp} + 2C_{Y\beta} (C_{l\phi})_1 - 2C_{Ll} C_{l\beta} \right]$$

$$F = \frac{1}{8\mu^2 \left(\frac{k_X}{b}\right)^2} \left\{ 2(C_{Yy'})_1 \left[ (C_{l\phi})_1 + (\overline{C_{l\phi}})_2 \right] \right\}$$

The derivative  $(\overline{C_{Y\phi}})_2$  enters into the calculations in such a way as to cancel a term involving  $(\overline{C_{l\phi}})_2$ .

#### GLIDER CHARACTERISTICS

The dimensional and mass characteristics of the Bristol tow-target glider "Skeet" for which the calculations were made are shown in the following table:

Wing area, square feet . . . . .	173.0
Horizontal tail area, square feet . . . . .	56.1
Vertical-tail area, square feet . . . . .	10.5
Wing span, feet . . . . .	34.4
Over-all length, feet . . . . .	29.3
Distance from center of gravity to towline- attachment points, feet . . . . .	15.0
Weight, pounds . . . . .	2976
Wing loading, pounds per square foot . . . . .	17.2
Radius of gyration about X-axis, feet . . . . .	5.3
Moment of inertia about X-axis, slug-feet <sup>2</sup> . . . . .	2596

Other factors that enter into the numerical calculations are:

$$C_{Y\beta} = -0.40$$

$$C_{l_p} = -0.40$$

$$\mu = 6.53$$

$$C_{l_\beta} = -0.012\Gamma_{\text{eff}}$$

$$\left(C_{Y_{y'}}\right)_1 = \frac{C_D}{a'}$$

$$\left(C_{l_\phi}\right)_1 = -\frac{C_D}{a'} \left(\frac{b_1}{b}\right)^2$$

$$\frac{k_X}{b} = 0.154$$

$$C_D = 0.0667 \quad (\text{at } C_L = 0.3)$$

$$C_D = 0.1047 \quad (\text{at } C_L = 0.75)$$

The value  $\left(C_{l_\phi}\right)_2$  is dependent upon glider displacements and is presented in figure 4.

#### CALCULATIONS AND RESULTS

Inasmuch as the calculation of the towline derivatives showed  $\left(C_{l_\phi}\right)_2$  and  $\left(C_{Y_\phi}\right)_2$  to be functions of glider displacements, the stability was investigated over a range of sidewise displacements by a step-by-step process. It was first necessary to assign some limiting value to the sidewise displacement  $y'$ . The towlines limit the sidewise travel to the length of the towline used but inspection of the model flight records indicated that these maximum values were never obtained in flight even with the most violent gusts or divergences. A study of these records indicated that, in almost all cases investigated for 1-, 2-, or 3-span towlines, the initial sidewise displacements of the glider center of gravity caused by gust disturbances did not exceed a value of 0.70 span. Since the towline conditions

Since the tunnel conditions simulate rather severe gust conditions in full-scale flight, this value was thought to be an adequate limit defining the maximum initial displacement likely to occur following a gust disturbance.

### Stability Boundaries

The theoretical requirements for dynamic stability of an airplane are that the coefficients of the stability equation and Routh's discriminant be positive. Negative values of the coefficients indicate divergent aperiodic modes; whereas a negative value of Routh's discriminant  $R$  (for positive coefficients) indicates an unstable periodic mode.

Stability boundaries separating stable from unstable regions may be defined by the equations:

$$C, E, \text{ or } F = 0 \text{ (aperiodic boundaries)}$$

$$R = BCE - E^2 - B^2F = 0 \text{ (periodic boundary)}$$

The periodic boundary  $R = 0$  was obtained by first evaluating the stability coefficients as defined in equation (27) for the desired glider condition in terms of  $(\overline{C_{l\phi}})_2$ . Routh's discriminant was set up and the value of  $(\overline{C_{l\phi}})_2$  calculated for  $R = 0$ . This value was then taken from the correct plot of  $(\overline{C_{l\phi}})_2$  against  $y'$  (fig. 4) and the value of  $y'$  obtained. The values of  $y'$  at which the stability coefficients  $F$  and  $C$  became zero were similarly obtained.

The aperiodic boundary  $E = 0$  is independent of the position derivatives and was obtained by calculating the value of the derivative  $C_{l\beta}$  necessary to cause the coefficient  $E$  to become zero.

The periodic boundary  $R = 0$  and the aperiodic boundaries  $C = 0$ ,  $E = 0$ , and  $F = 0$  are given on the charts of effective dihedral  $\Gamma_{\text{eff}}$  plotted against side-wise displacement in figures 5, 6, and 7 for two values of lift coefficient and for 1-, 3-, and 3-span towlines. Stability ratings from flight data of reference 1 are

also given on these figures for different values of effective dihedral angle. The geometric dihedral angle was converted to effective dihedral angle by means of data from unpublished full-scale-tunnel tests of the glider made at LMAL. The full-scale data indicated that the effective dihedral angle of the test glider was  $1.5^\circ$  lower than its geometric dihedral angle for a lift coefficient of 0.30 and  $1.5^\circ$  higher than its geometric dihedral angle for a lift coefficient of 0.75.

### Stability Roots

The stability boundaries, although defining the various stability regions, give no quantitative indication of the variation of stability within a given region. These characteristics may be obtained by factoring the stability equation for its roots  $\lambda_1$ ,  $\lambda_2$ ,  $\lambda_3$ , and  $\lambda_4$  and using these roots to determine the period of the lateral oscillations and the time to damp to one-half amplitude for the oscillatory and aperiodic modes.

The period in seconds of the periodic modes  $\lambda_3$  and  $\lambda_4$  was obtained by the formula

$$P = \frac{2\pi}{d} \frac{b}{V}$$

where  $d$  is the imaginary portion of the complex roots

$$\lambda_3, \lambda_4 = c \pm id$$

The time to damp to one-half amplitude in seconds was calculated from the formula

$$\begin{aligned} t_{1/2} &= - \frac{\log_e 0.5}{c} \frac{b}{V} \\ &= - \frac{0.693}{c} \frac{b}{V} \end{aligned}$$

where  $c$  is either the real portion of the complex roots for the oscillatory mode or the real root  $\lambda_1$  or  $\lambda_2$  defining the aperiodic modes.

The reciprocal of the time to damp to one-half amplitude has been used herein to express damping. This procedure was followed because it was desired to express the degree of stability as a direct rather than as an inverse function of the ordinate. Peak positive ordinates consequently indicate maximum damping and negative ordinates indicate negative (unstable) damping.

The aperiodic mode  $\lambda_1$  represents a heavily damped convergence that is always stable and is little affected by changes in glider or towline configuration. An example of the damping characteristics of this mode is presented in figure 8 for the condition with 2-span towlines to illustrate its general nature. The mode  $\lambda_2$  is the governing aperiodic mode and hence determines the aperiodic characteristics of the glider.

Complete calculations of the period and damping characteristics have been made for tow with 1-, 2-, and 3-span towlines at two values of lift coefficient and two values of sidewise displacement. Representative results are presented in figures 9 to 15. Experimental values of the period of the lateral oscillations determined in the tests reported in reference 1 and corrected to full-scale values are also given on the figures for purposes of comparison.

## DISCUSSION

### Effect of Dihedral Angle

An analysis of the stability charts (figs. 5 to 7) indicates that dihedral angle is an important factor in the determination of the stability of the glider. The only satisfactory stability region is that in which the effective dihedral angle ranges from small to moderately large positive values. At angles above this region (indicated by the dashed line on charts) the glider may be stable or unstable depending upon its initial sidewise displacement, and at angles below this region unstable oscillations and divergences are encountered.

The stability charts indicate a close degree of correlation between the theoretical and the flight results. The dihedral range of the various stability regions indicated by theory is corroborated by the flight tests and

stability reversal in flight occurs at approximately the same effective dihedral as that indicated by the stability boundaries.

L-572

Typical variations of the period of the periodic mode and the damping characteristics of the periodic and aperiodic modes are presented in figures 9, 10, and 11. These figures further amplify the conclusions drawn from the boundary charts and indicate that a high degree of stability is obtained at small positive dihedral angles. As shown by figure 9, maximum damping of the oscillatory mode exists for these dihedral angles. Any increase or decrease of dihedral away from these small positive values results in lighter damping of the oscillatory mode and eventually results in oscillatory instability.

Figure 10 shows that an increase in the period of the lateral oscillations occurs with reduction of effective dihedral angle, resulting in long-period oscillations for small negative dihedral angles. These long-period oscillations occur in an unstable oscillatory region and, hence, are likely to have the appearance of truly divergent modes that exist at more negative dihedral angles. These characteristics may account for the divergence ratings given the flight test made with small negative effective dihedral angles.

The point of peak stability noted for low positive dihedral angles in the theoretical analysis is in agreement with the flight test data in reference 1, in which the steadiest and most stable flights occurred at small positive dihedral angles. As predicted by the theoretical analysis, divergent conditions were encountered in the flight tests for negative values of effective dihedral. Reasonably close quantitative agreement was obtained for the period of the oscillatory mode as shown in figure 10, and both investigations indicated an increase in period with decrease in effective dihedral angle.

#### Effect of Sidewise Displacement

Figures 9 and 11 illustrate the adverse effect of sidewise displacement upon the stability characteristics of the glider. A decrease in the damping of all stability modes accompanies sidewise displacement. Although this effect is small for small positive dihedral angles, it becomes the predominant factor in the determination of

the stability for large positive dihedrals and eventually causes oscillatory instability or divergent flight. These results explain certain phenomena previously encountered in the flight tests reported in reference 1 for flights with large dihedral angles. During the tests the model would fly quite satisfactorily for some period of time at large dihedral angles before unstable oscillations developed.

In order to obtain more flight data on the effect of sidewise displacement, additional flight tests have since been made in which a model equipped with remote controls was attached to a tunnel support by means of a dyadic towline system. This model, although larger and heavier than the original test model, portrayed the same essential variation of stability with dihedral angle as the original model. The model was then flown at level tow and aileron control disturbances were introduced during the flight. In these flights the model would fly satisfactorily in the center position and would even damp out light control disturbances. For large control disturbances involving large sidewise displacements, however, unstable oscillations would occur. These tests confirmed the theoretical premise that the stability of the glider at high values of effective dihedral angle is largely dependent upon initial sidewise displacement. The results indicate that gusty atmospheric conditions may induce instability in flights when the dihedral angle of the glider is large; whereas complete stability would exist for smoother air-flow conditions. The advantages of small dihedrals are consequently again emphasized.

#### Effect of Towline Length

The effect of towline length upon the period and damping characteristics of the glider is illustrated in figures 12, 13, and 14. These figures indicate that increasing the length of the towlines seriously lessened the degree of damping of the oscillatory and aperiodic modes. A reduction of stability was evidenced for all dihedral angles for lengthened towlines, and the peak damping of the oscillatory mode for 3-span towlines was approximately 50 percent of that obtained with 1-span towlines. The damping of the aperiodic mode was also seriously lessened by increase in length of the towlines, particularly for the higher value of lift coefficient. This effect probably accounts for the discrepancy between



L-372

the flight results and the calculated results for a lift coefficient of 0.75 and 3-span towlines. (See fig. 7.) Apparently, the damping of the aperiodic mode for these flights was so low, even though positive, that sustained flights could not be made.

In general, increasing the towline length resulted in a slight increase in the period of the lateral oscillations.

The flight tests of reference 1 were in good agreement with the theoretical study with regard to the effect of towline length. The lessening of the glider stability and the more or less constant nature of the period of the lateral oscillations with increased towline length were noted throughout the flight tests.

#### Effect of Lift Coefficient

The theoretical investigation showed that increasing the lift coefficient from 0.30 to 0.75 slightly increased the period of the oscillatory mode and reduced the damping of both the oscillatory and aperiodic modes. This effect of increased lift coefficient upon the period of the lateral oscillations is illustrated in figure 14 and upon the damping characteristics is shown in figures 15 and 16.

Although for 1-span towlines only moderate effects of lift coefficients were evident, for longer towlines the adverse effects of high values of lift coefficient became more serious. Because of the lower stability associated with the larger value of lift coefficient, it was indicated that flights at large positive dihedrals would become unstable with sidewise displacements smaller than those displacements inducing instability at the lower value of lift coefficient. This trend was accentuated with increased towline length until, with 3-span towlines, complete instability occurred at a value of  $14^\circ$  effective dihedral for all values of sidewise displacement, as shown in figure 7.

The flight data were in good agreement with the theoretical results. The reduction in stability with increase of lift coefficient in the flight tests was slight for 1-span towlines but became noticeable and serious for longer towlines.

### Effect of Lift-Drag Ratio

The results of the theoretical survey as shown in figure 17 revealed a decided advantage of low lift-drag ratios with respect to the damping of the oscillatory mode. These data apply only to zero sidewise displacement but similar trends occurred for other values of displacement.

The results indicate that greatest stability will be obtained at low values of lift-drag ratio. The damping of lateral oscillations reached a maximum at a lift-drag ratio of 4 for the glider investigated. Increasing this ratio to a higher value resulted in less stability for all dihedral angles although as would be expected, this effect was least pronounced for small positive values of dihedral angle.

The highly advantageous effect of spoilers, which reduce lift-drag ratio, as reported in the flight tests of reference 1 may be seen to confirm these data.

### CONCLUSIONS

A theoretical study of the lateral stability of a glider towed by twin parallel towlines indicates the following conclusions:

1. A dyadic system of parallel towlines that imposes a restraint in yawing will provide satisfactory inherent stability for a pilotless towed glider.
2. The lateral stability will be chiefly influenced by the dihedral angle of the wing. A maximum of stability will exist over a range of small positive values of effective dihedral. Any variation of dihedral from this range will lead to progressively less stability and will eventually result in unstable oscillations or divergences.
3. Gusty atmospheric conditions, which result in large sidewise displacements of the glider relative to the tug, will reduce the stability inherent in the tow system. This effect will be greatest for large positive values of effective dihedral.

4. Long towlines will decrease the lateral stability of the glider although stable satisfactory flight will still be obtainable for towlines up to three spans.

5. Increasing the lift coefficient of the glider will reduce the lateral stability for all conditions. This effect will be slight for short towlines but will increase in magnitude with long towlines.

6. Low lift-drag ratios will increase the lateral stability of the glider.

Langley Memorial Aeronautical Laboratory,  
National Advisory Committee for Aeronautics,  
Langley Field, Va.

#### REFERENCES

1. Pitkin, Marvin, and McKinney, Marion O., Jr.: Flight Tests of a Glider Model Towed by Twin Parallel Towlines. NACA RB No. 3D30, April 1943.
2. Zimmerman, Charles H.: An Analysis of Lateral Stability in Power-Off Flight with Charts for Use in Design. Rep. No. 589, NACA, 1937.

1. The first part of the report deals with the general situation of the country and the progress of the work during the year.

2. The second part of the report deals with the results of the work done during the year and the progress of the various projects.

3. The third part of the report deals with the financial position of the organization and the results of the financial work.

4. The fourth part of the report deals with the administrative work done during the year and the progress of the various projects.

CONCLUSION

1. The work done during the year has been satisfactory and the progress of the various projects has been good.

2. The financial position of the organization is satisfactory and the results of the financial work are good.

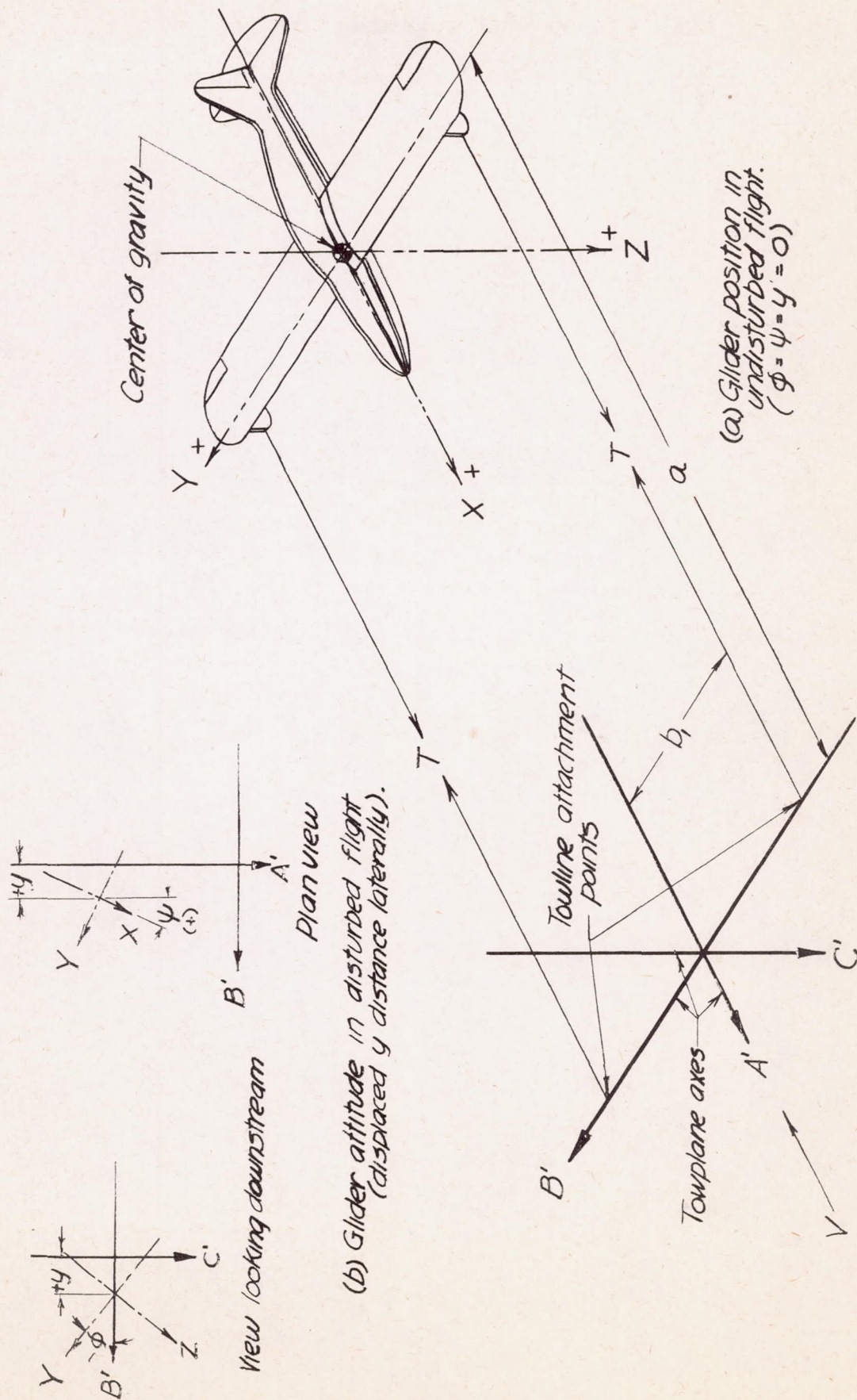
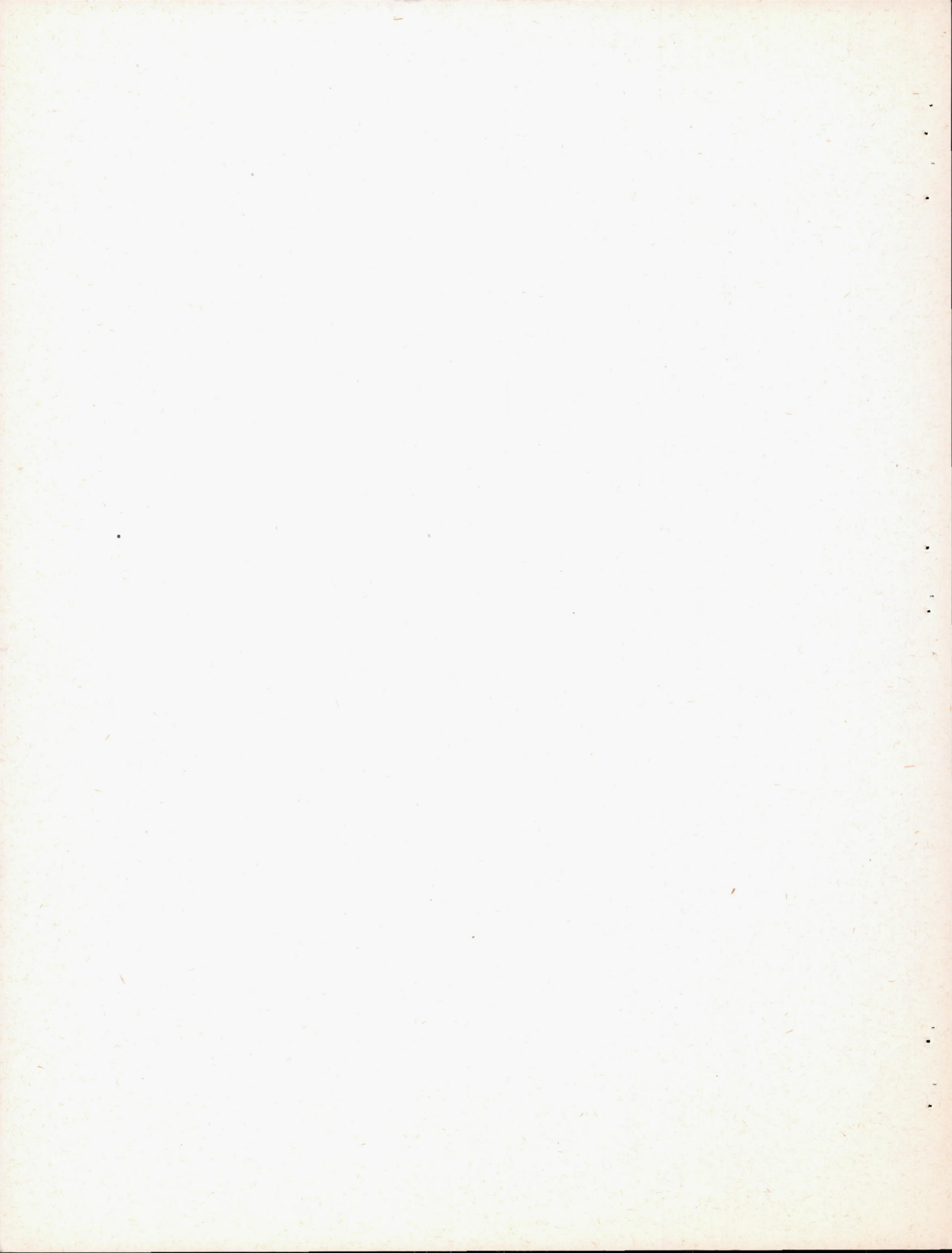


Figure 1.- Schematic layout of dyadic towline system. Level tow.



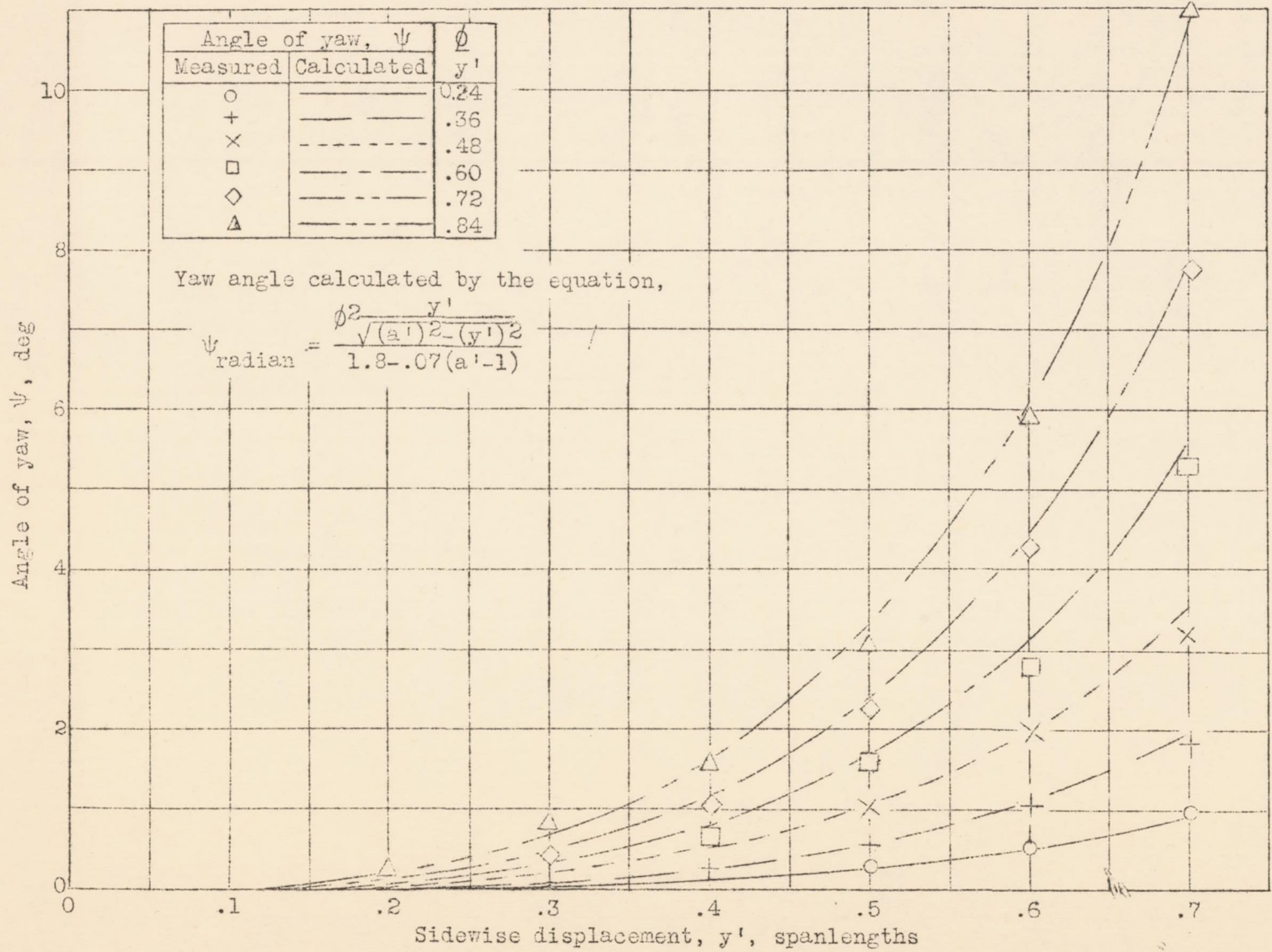


Figure 2.- Comparison between calculated and measured values of yaw induced by glider attitude. .1-span towlines.

Vertical axis label: ...

Horizontal axis label: ...



Vertical text label: ...

Vertical text label: ...

1	2	3	4	5	6	7	8	9	10
1	2	3	4	5	6	7	8	9	10
2	3	4	5	6	7	8	9	10	11
3	4	5	6	7	8	9	10	11	12
4	5	6	7	8	9	10	11	12	13
5	6	7	8	9	10	11	12	13	14
6	7	8	9	10	11	12	13	14	15
7	8	9	10	11	12	13	14	15	16
8	9	10	11	12	13	14	15	16	17
9	10	11	12	13	14	15	16	17	18
10	11	12	13	14	15	16	17	18	19



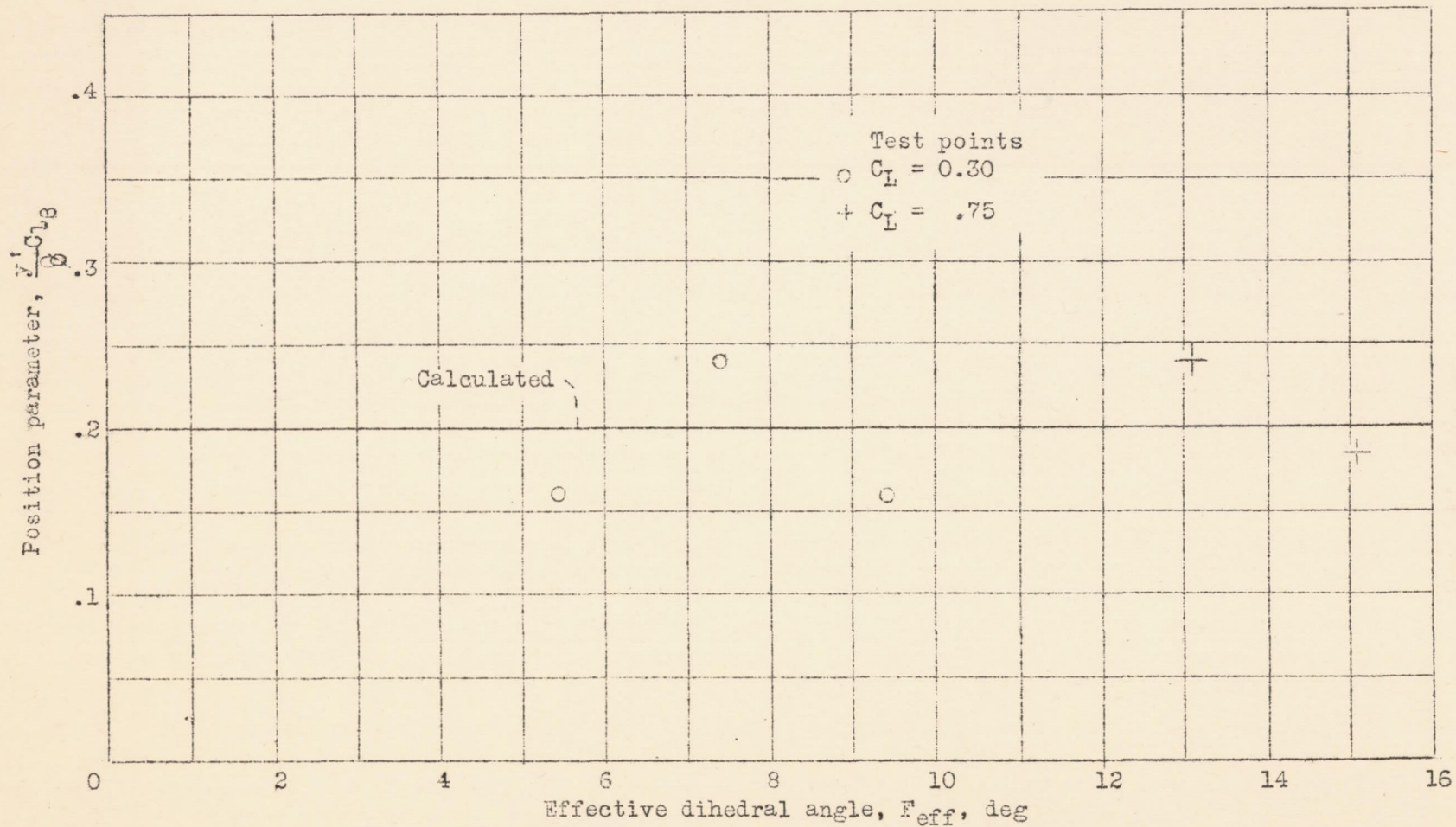
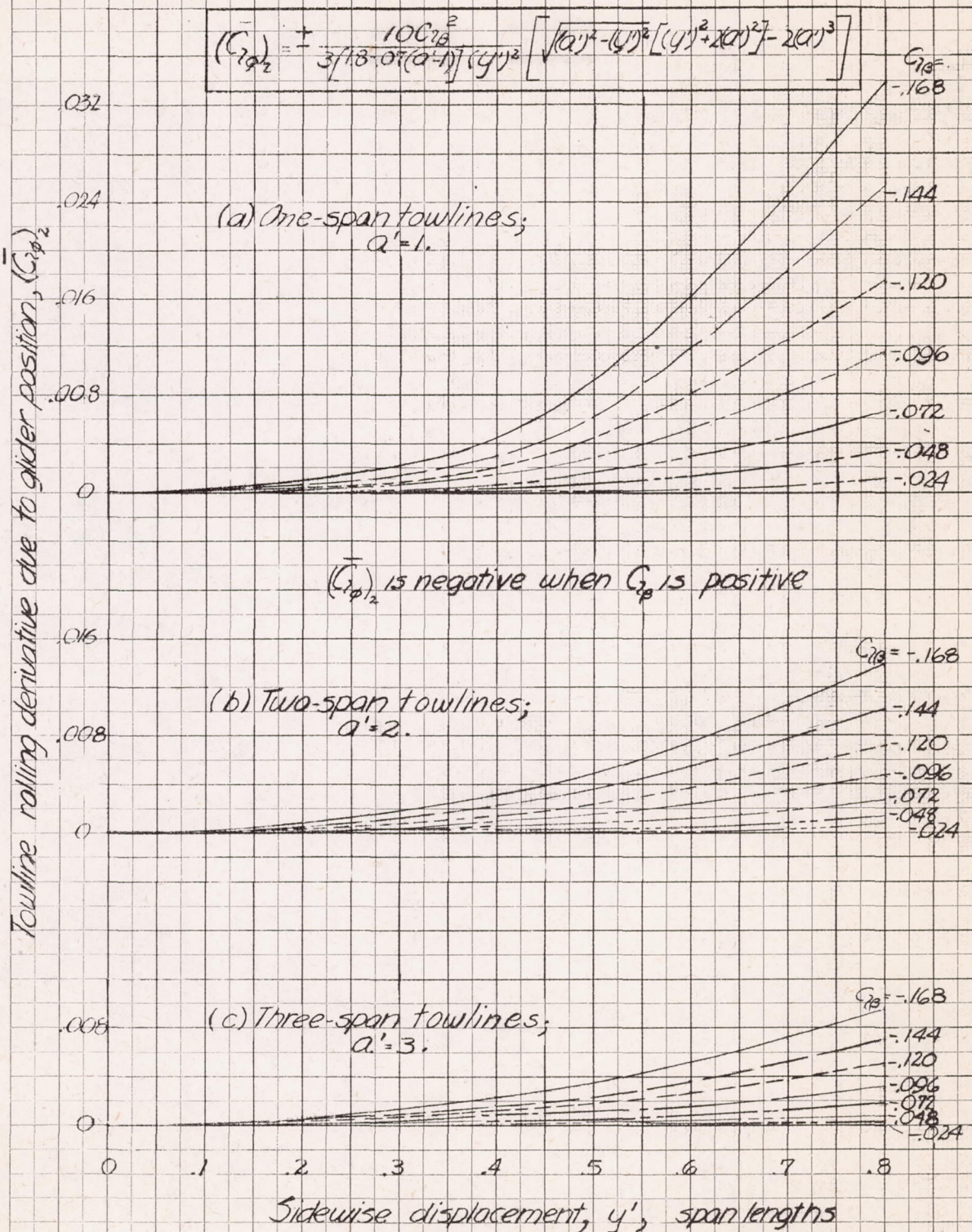


Figure 3.- Comparison of calculated and experimental values of the position parameter,  $\frac{y^1}{\phi} C_{L\beta}$ .





NATIONAL ADVISORY  
COMMITTEE FOR AERONAUTICS

Figure 4. Towline rolling derivative due to glider position for 1-, 2-, and 3-span towlines.

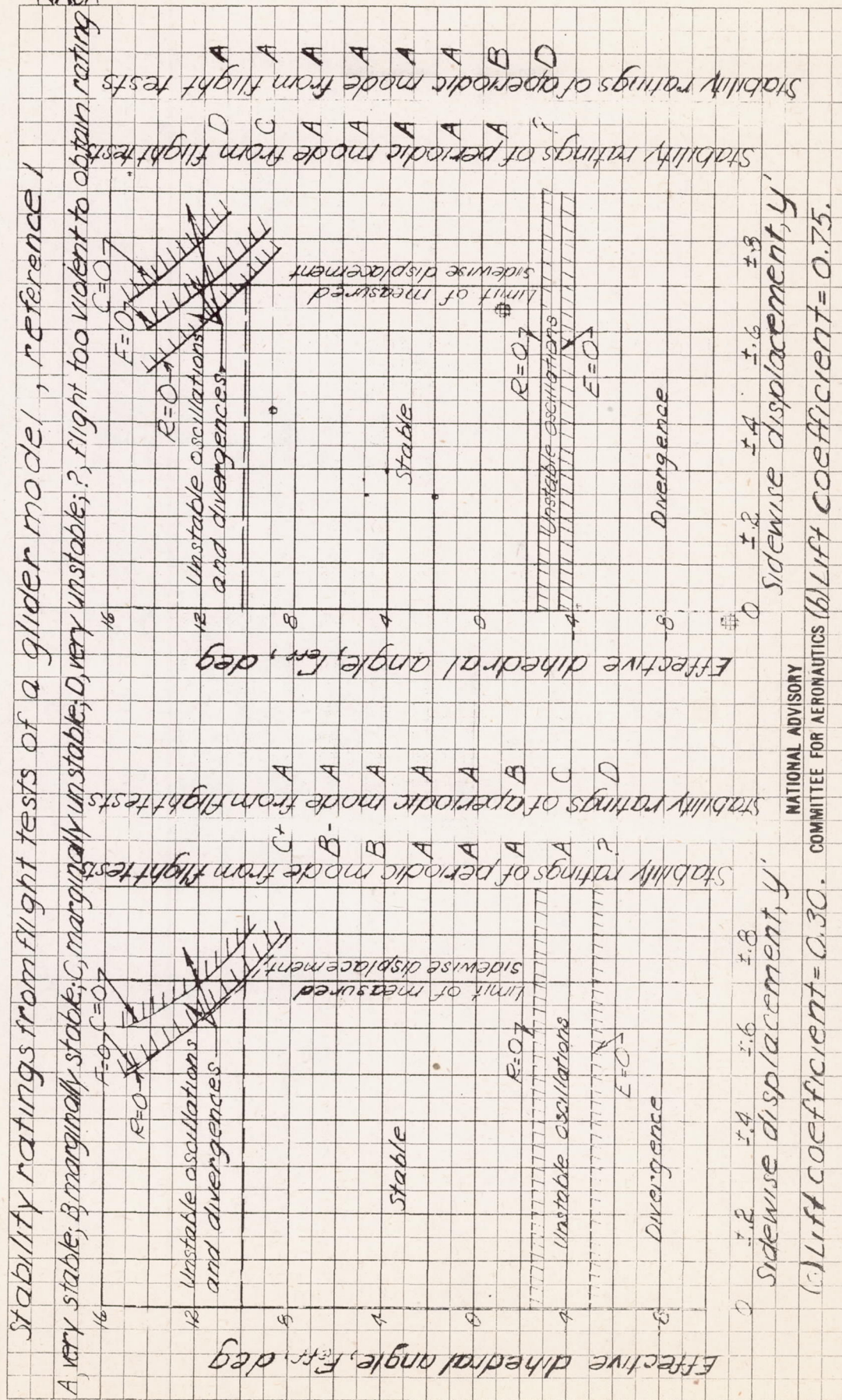
L-372



Stability ratings from flight tests of a glider model, reference 1

A, very stable; B, marginally stable; C, marginally unstable; D, very unstable; ?, flight too violent to obtain rating

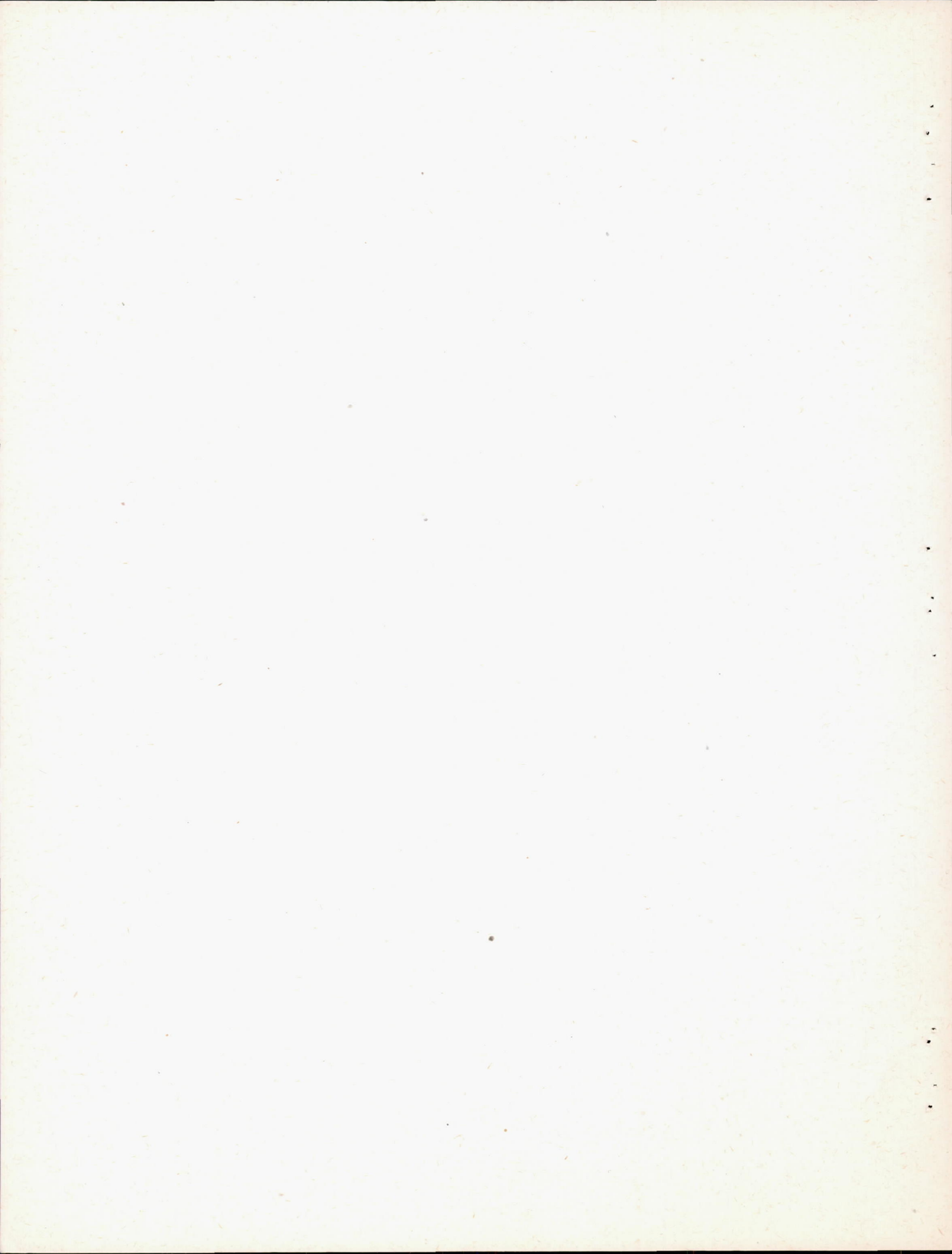
NACA



NATIONAL ADVISORY COMMITTEE FOR AERONAUTICS

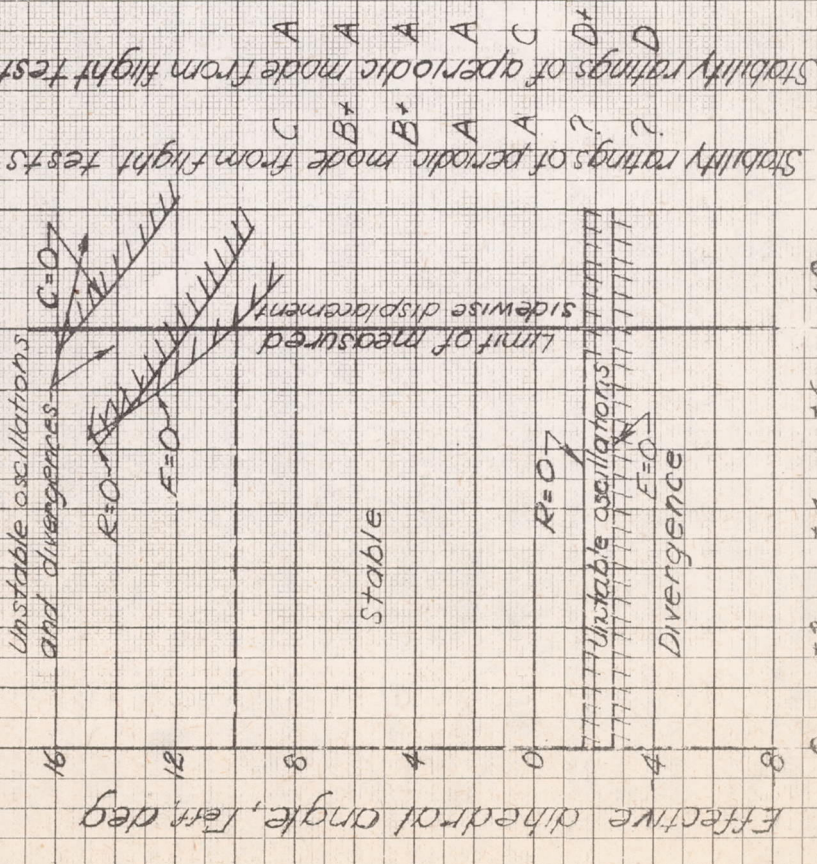
(c) Lift coefficient = 0.30. (b) Lift coefficient = 0.75.

Figure 5 - Calculated stability boundaries correlated with stability ratings from flight tests of a glider model with 1-span towlines.

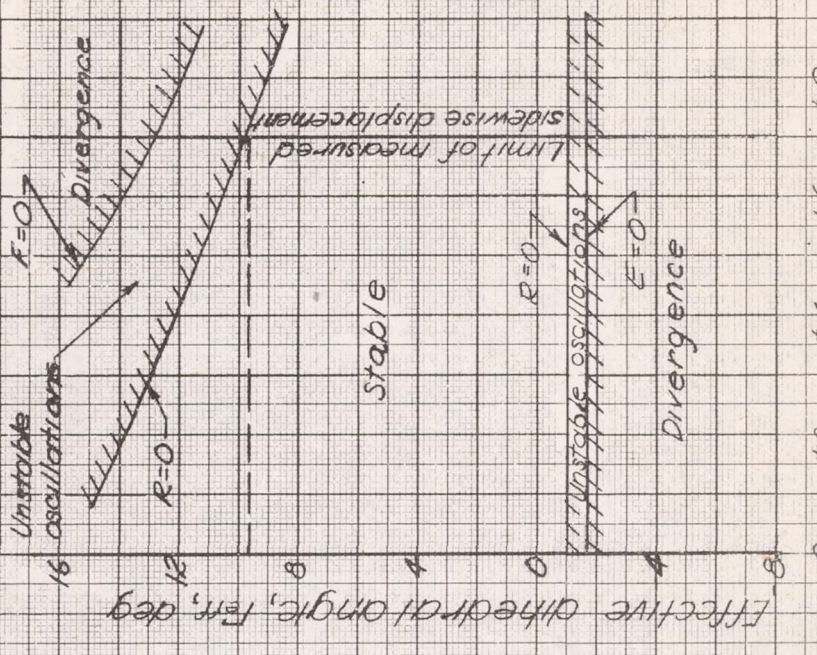


Stability ratings from flight tests of a glider model, reference 1

A, very stable; B, marginally stable; C, marginally unstable; D, very unstable; P, flight too violent to obtain rating



(a) Lift coefficient = 0.30. Sidewise displacement,  $y'$



(b) Lift coefficient = 0.75. Sidewise displacement,  $y'$

Figure 6. - Calculated stability boundaries correlated with stability ratings from flight tests of a glider model with 2-span towlines.

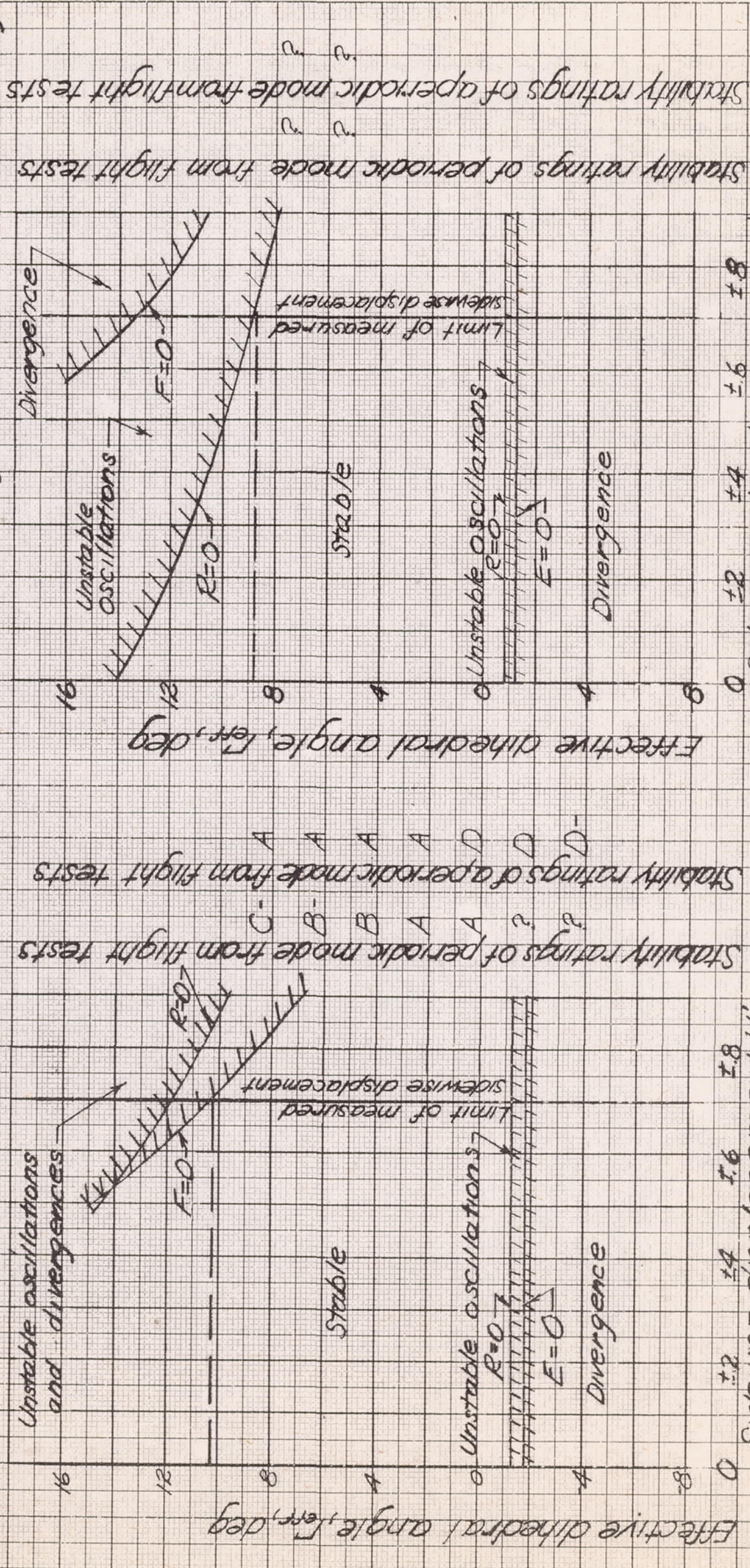
NATIONAL ADVISORY  
COMMITTEE FOR AERONAUTICS





Stability ratings from flight tests of a glider model, reference 1

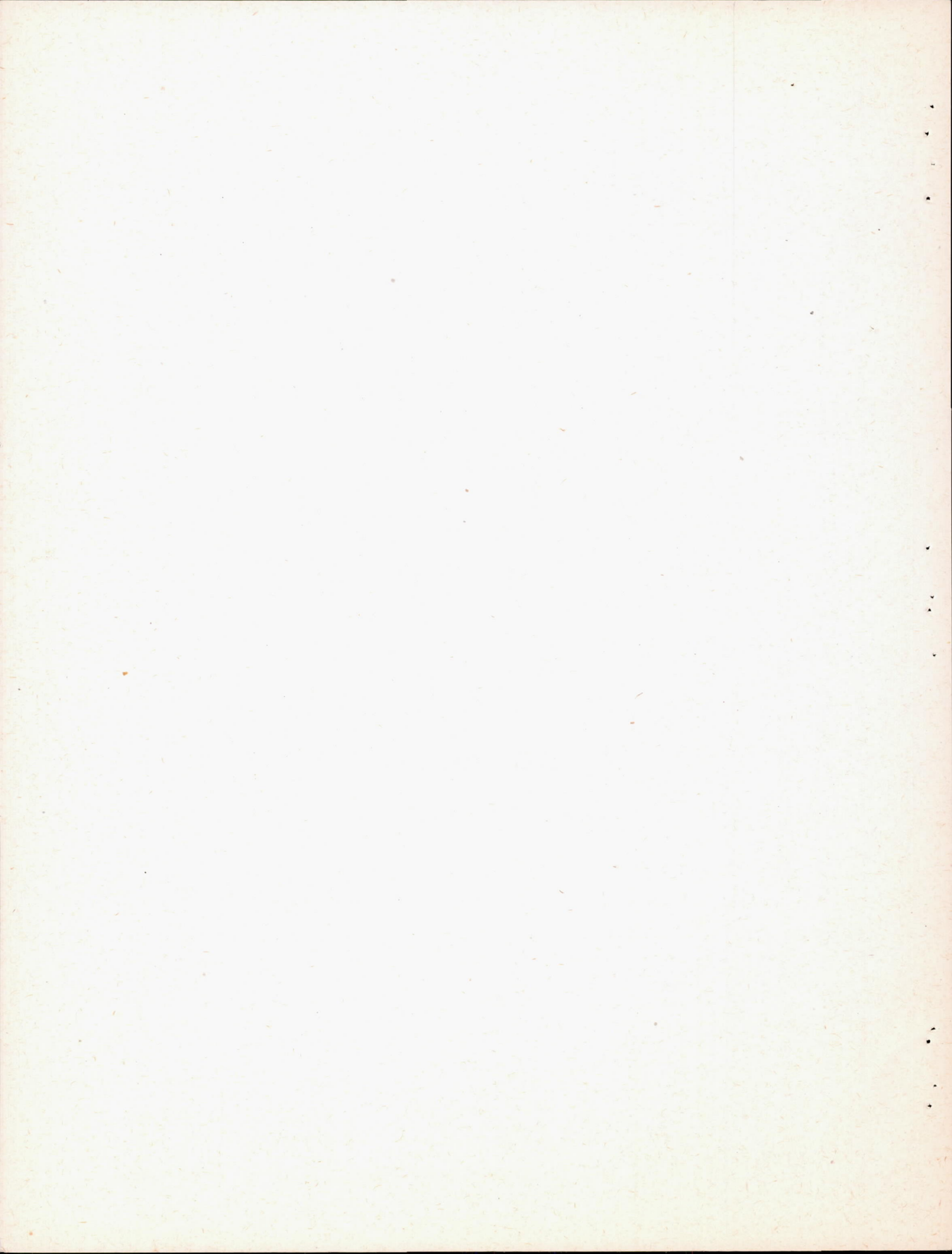
A, very stable; B, marginally stable; C, marginally unstable; D, very unstable; P, flight too violent to obtain rating



NATIONAL ADVISORY COMMITTEE FOR AERONAUTICS

(a) Lift coefficient = 0.30. (b) Lift coefficient = 0.75.

Figure 7 - Calculated stability boundaries correlated with stability ratings from flight tests of a glider model with 3-span towlines.



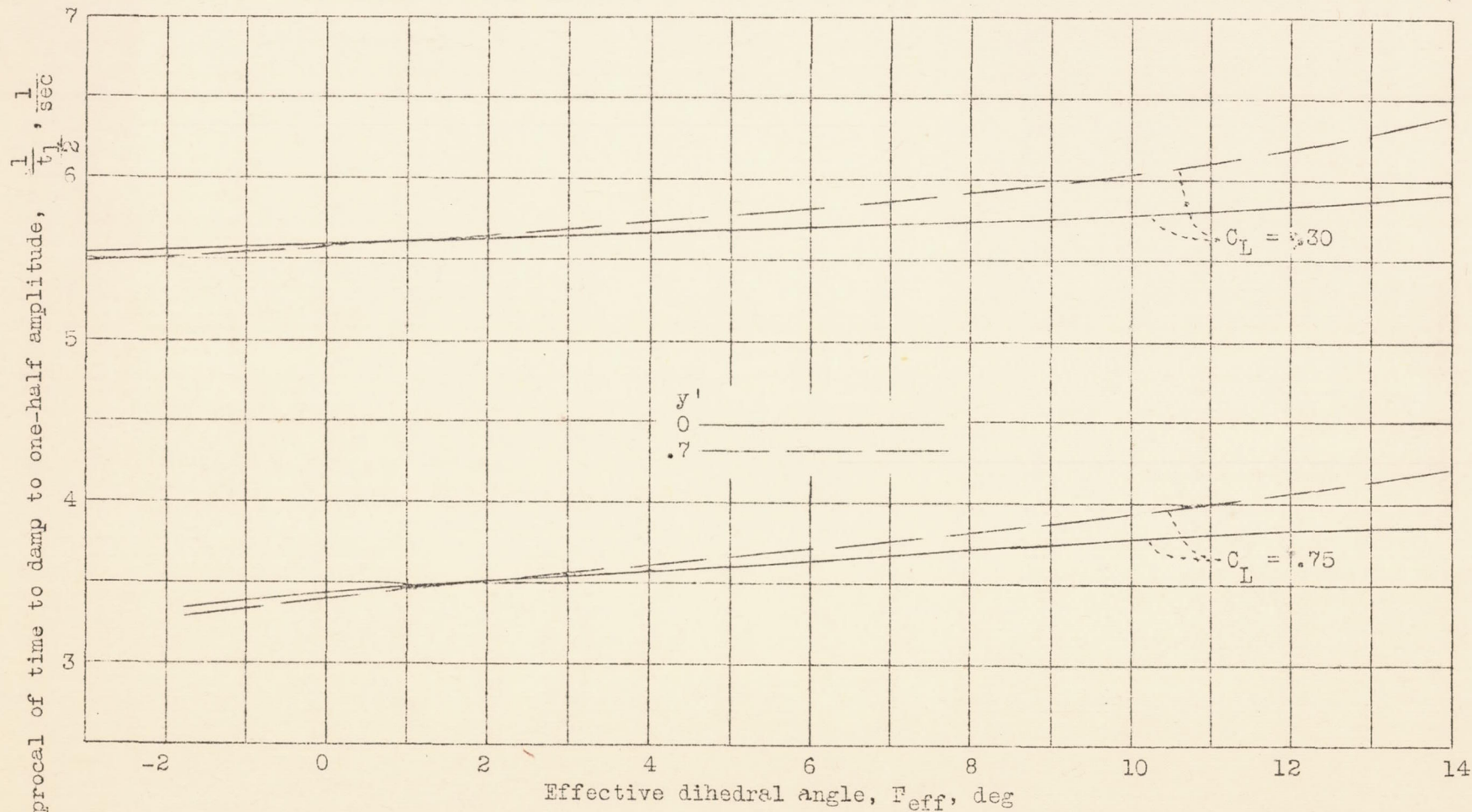
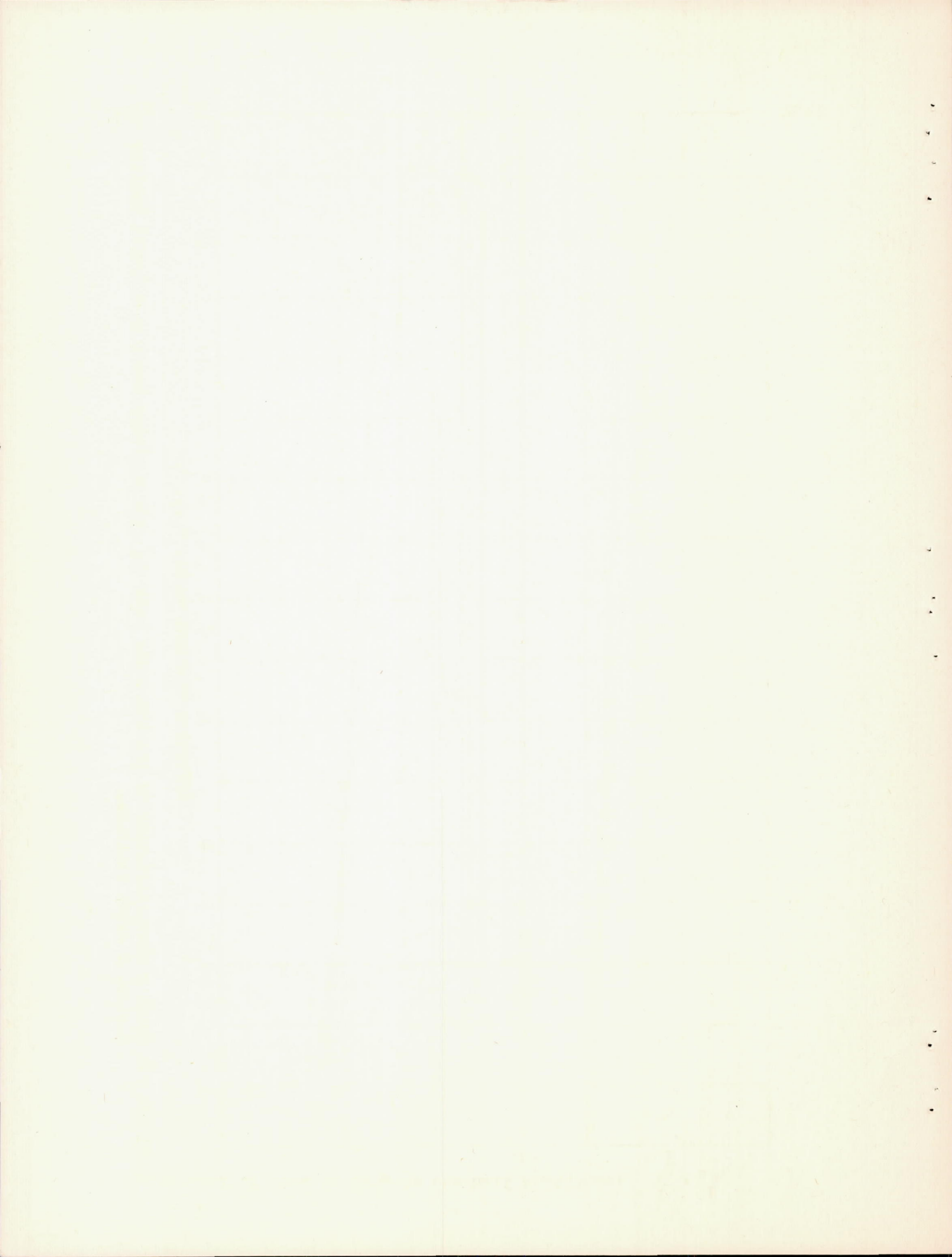


Figure 8.- Damping characteristics of the aperiodic mode  $\lambda_1$  for a glider towed by a dyadic towline system. 2-span towlines.



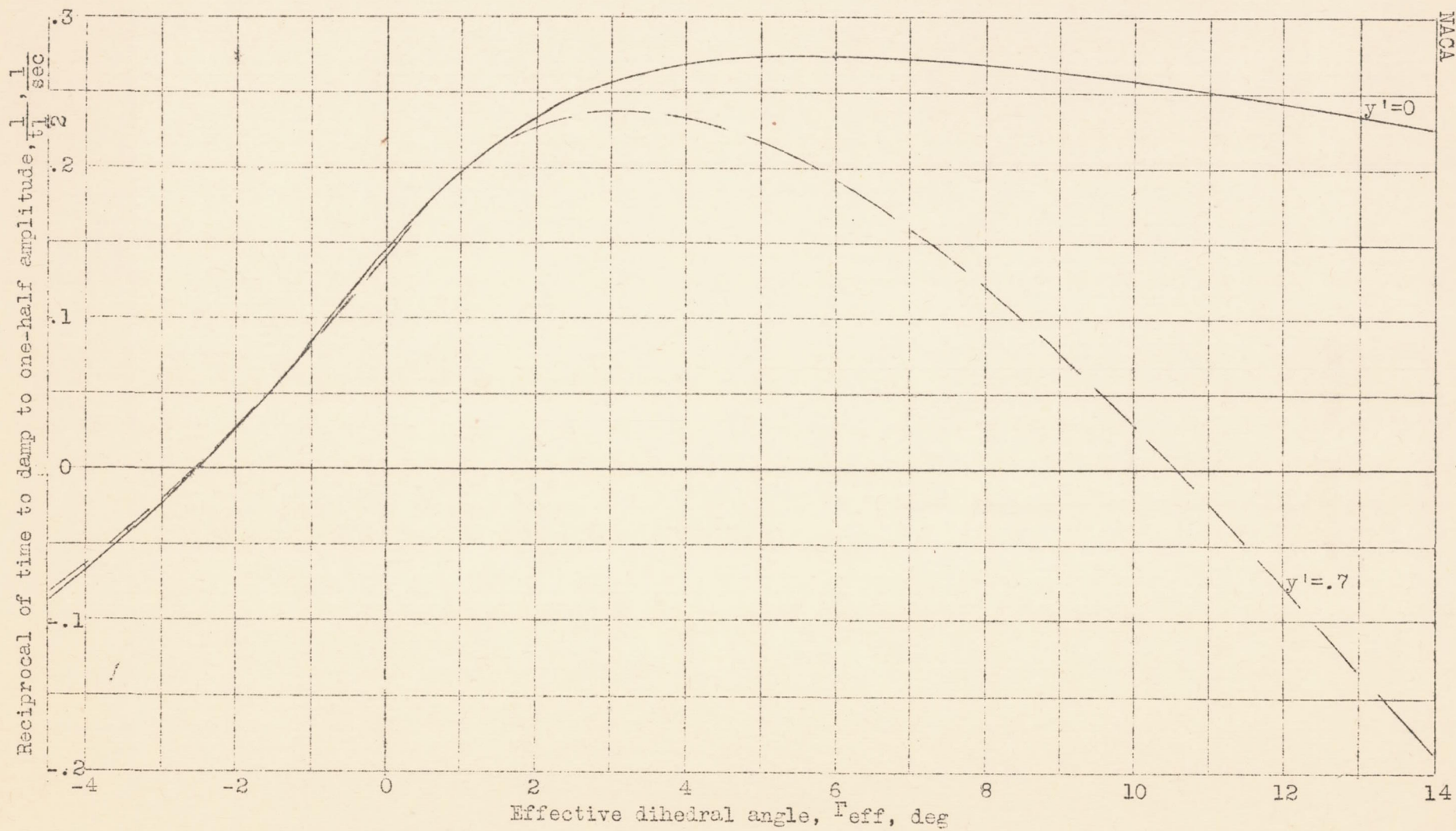
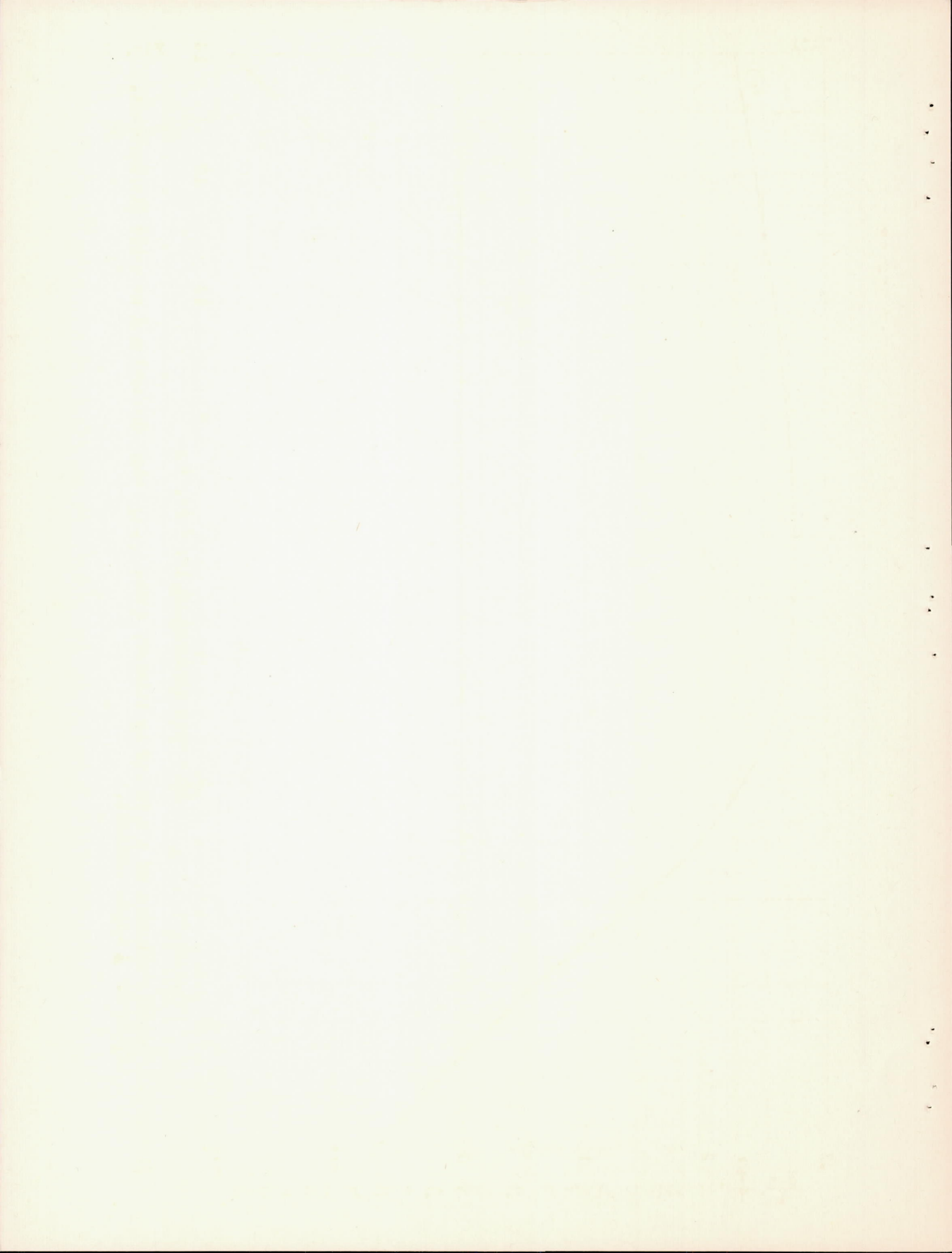


Figure 9.- Typical variation of damping of oscillatory modes  $\lambda_3, \lambda_4$  with dihedral and sidewise displacement.  $C_L = 0.30$ .  $\frac{1}{\tau}$  - span towlines.



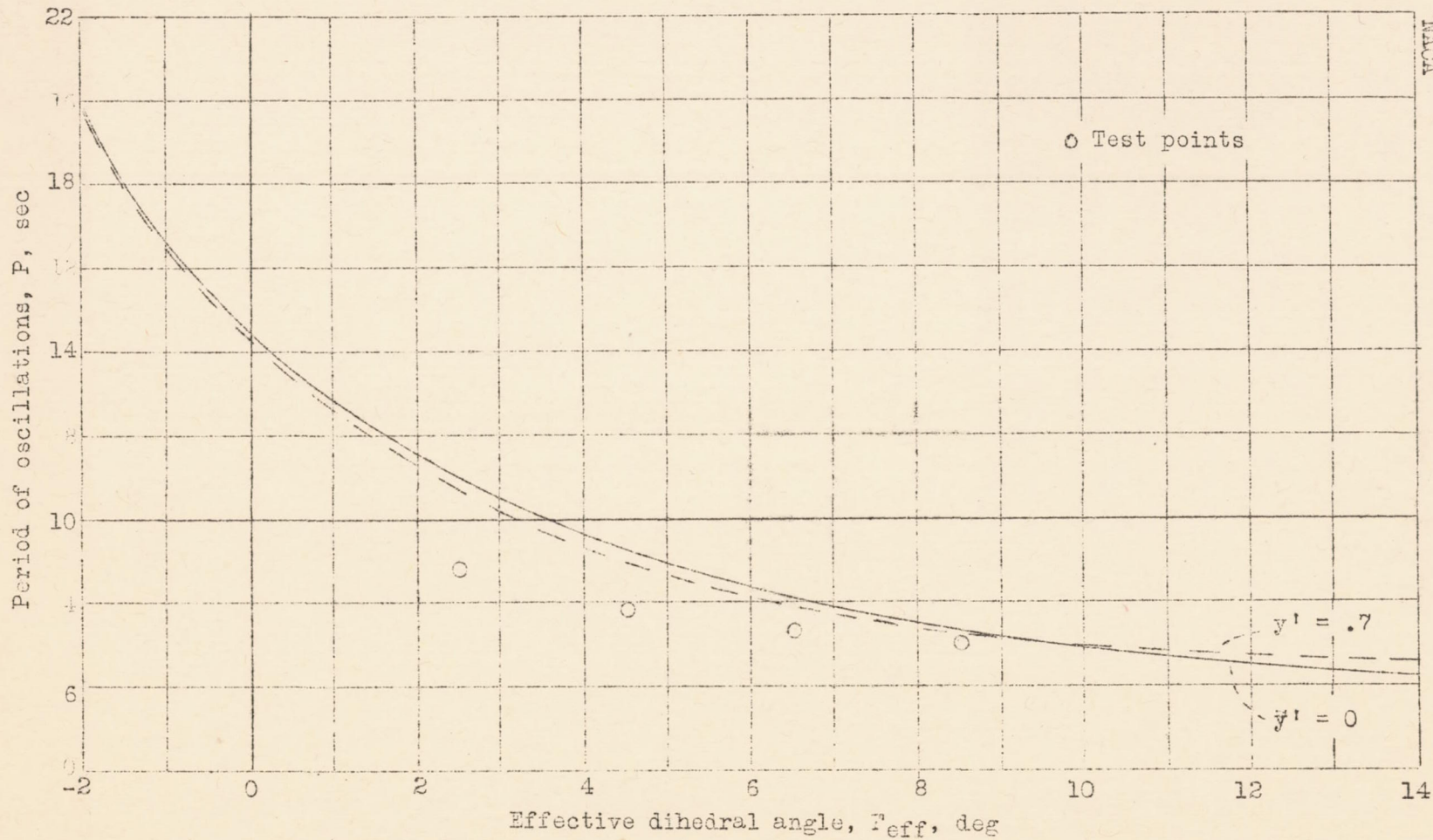


Figure 10.- Typical variation of period of oscillatory mode  $\lambda_3$ ,  $\lambda_4$  with dihedral and sidewise displacement.  $C_L = 0.30$ , 1-span towlines.

CE 1017

1952

RECEIVED THE BUREAU OF THE DISTRICT ATTORNEY

THE STATE OF CALIFORNIA  
COUNTY OF SAN DIEGO  
IN SENATE  
JANUARY 15 1952  
BY THE DISTRICT ATTORNEY  
JAMES H. HARRIS  
DISTRICT ATTORNEY  
SAN DIEGO, CALIFORNIA



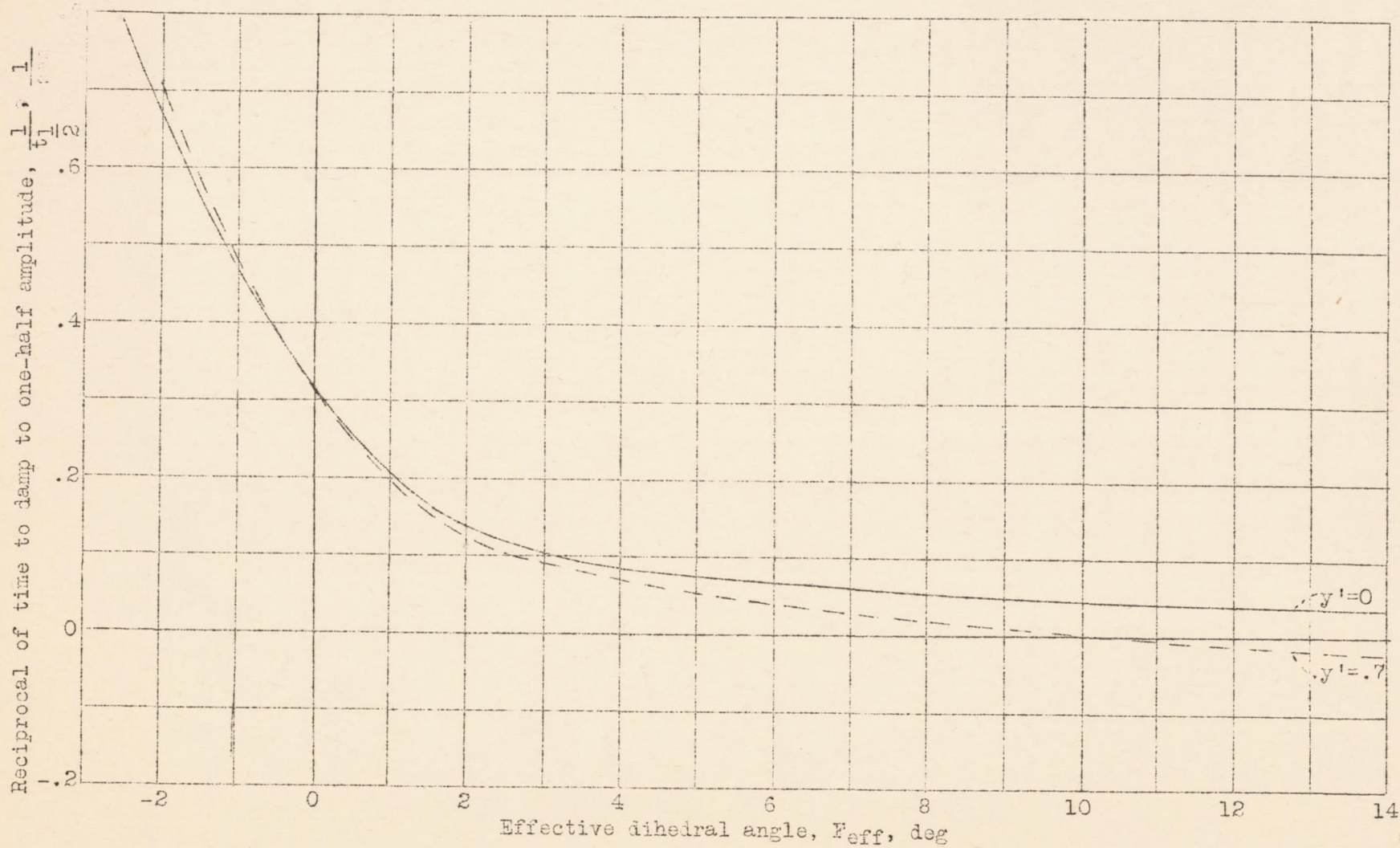


Figure 11.- Typical variation of damping of aperiodic mode  $\lambda_2$  with dihedral and sidewise displacement.  
 $C_L = .30$ . 2-span towlines.

At the time of the ...

... ..

... ..

... ..

... ..

... ..

... ..

... ..

... ..

... ..

... ..

... ..

... ..

... ..

... ..

... ..

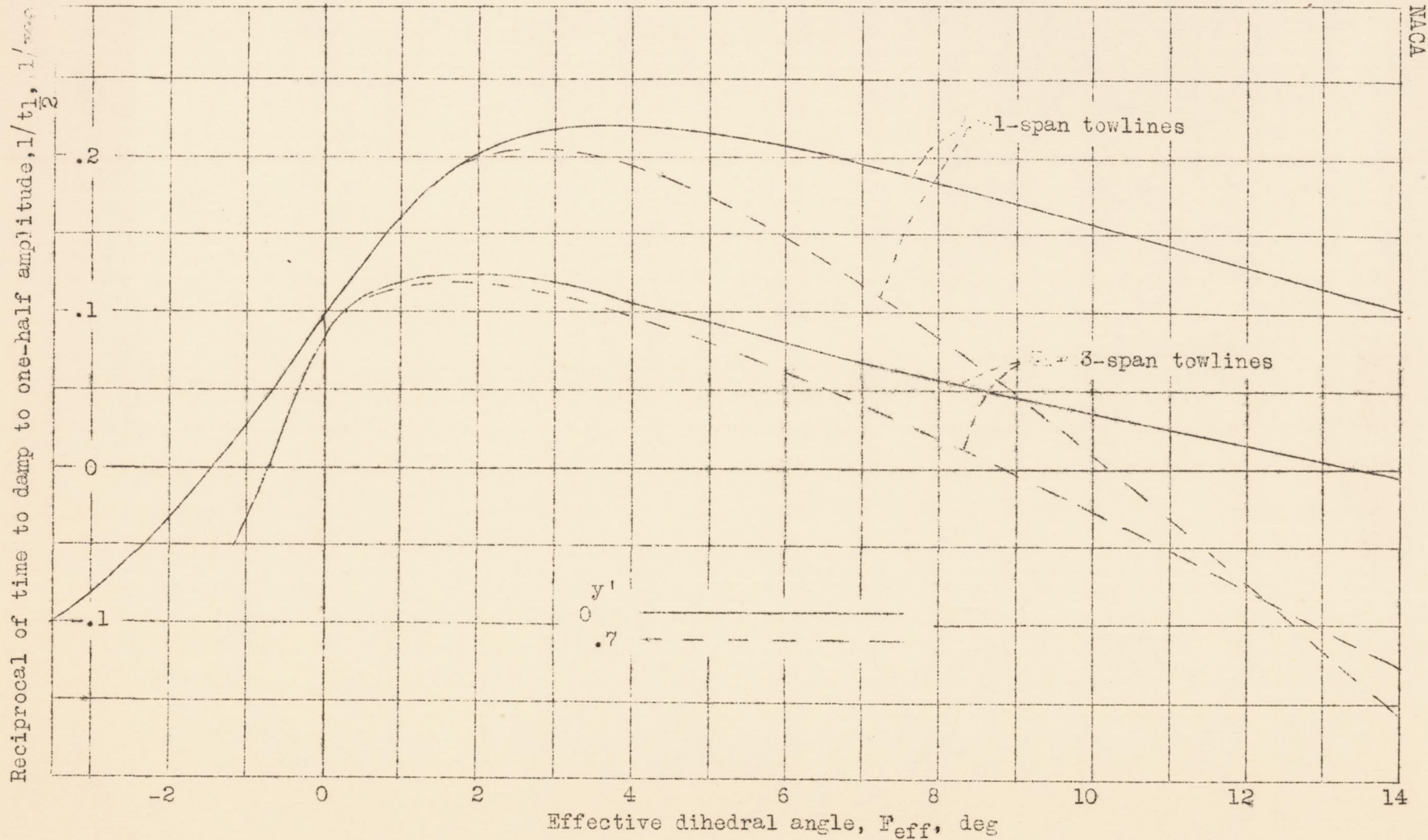


Figure 12.- Effect of towlength on the damping of the periodic modes  $\lambda_3, \lambda_4$  of a glider towed by a dyadic tow system.  $C_L = 0.75$ .

Part 100 of the ...  
... of the ...



11

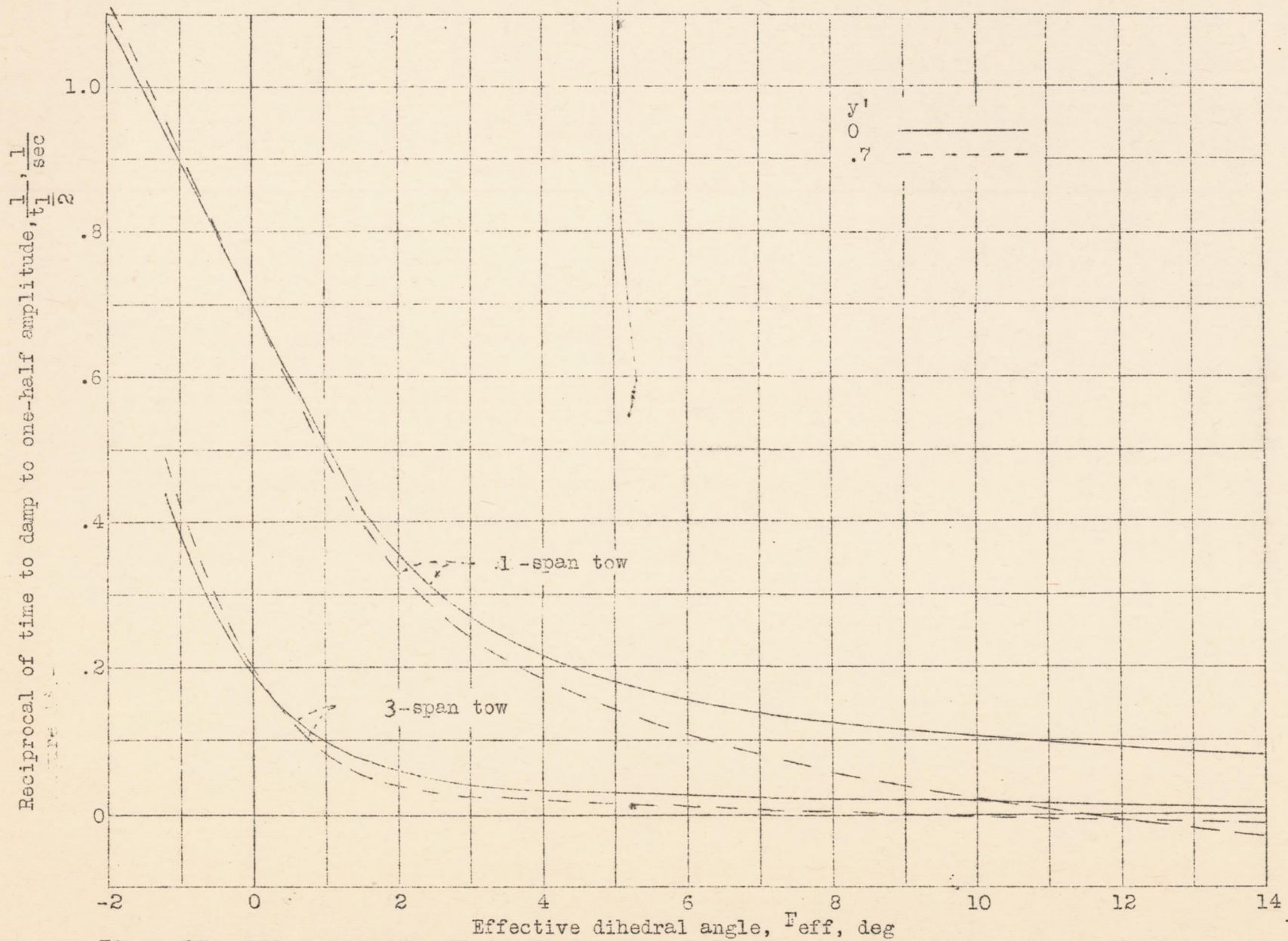


Fig. 13

Figure 13.- Effect of towlength on the damping of the aperiodic mode  $\lambda_2$  of a glider towed by a dyadic tow system.  $C_L=0.75$ .

1875

Office of the Surveyor General of the Territory of New Mexico  
Santa Fe, N.M., July 10, 1875



Survey of the land of the Territory of New Mexico

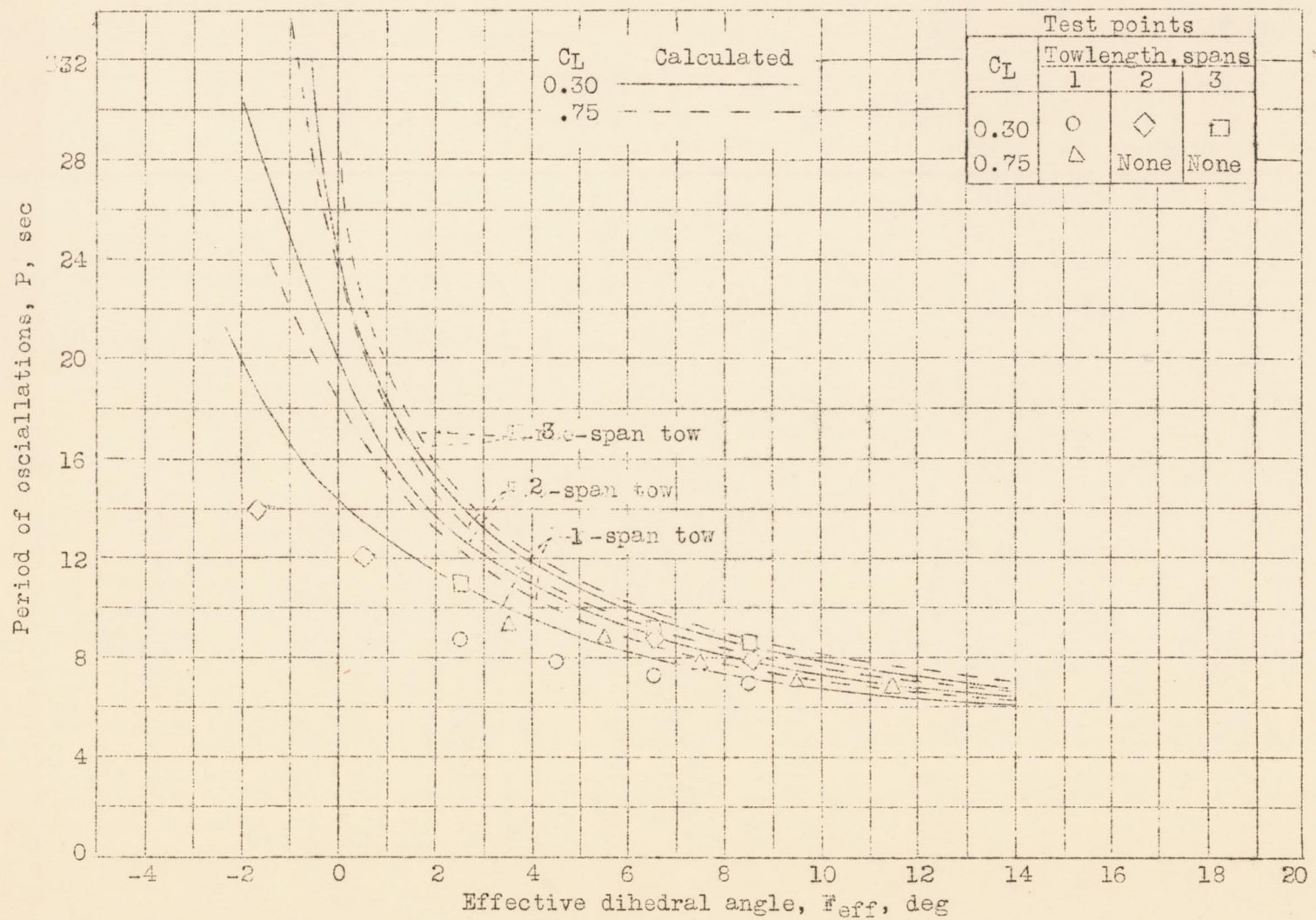


Figure 14.- Effect of towlength on the period of the oscillatory mode of a glider towed by a dyadic tow system.  $y' = 0$ .





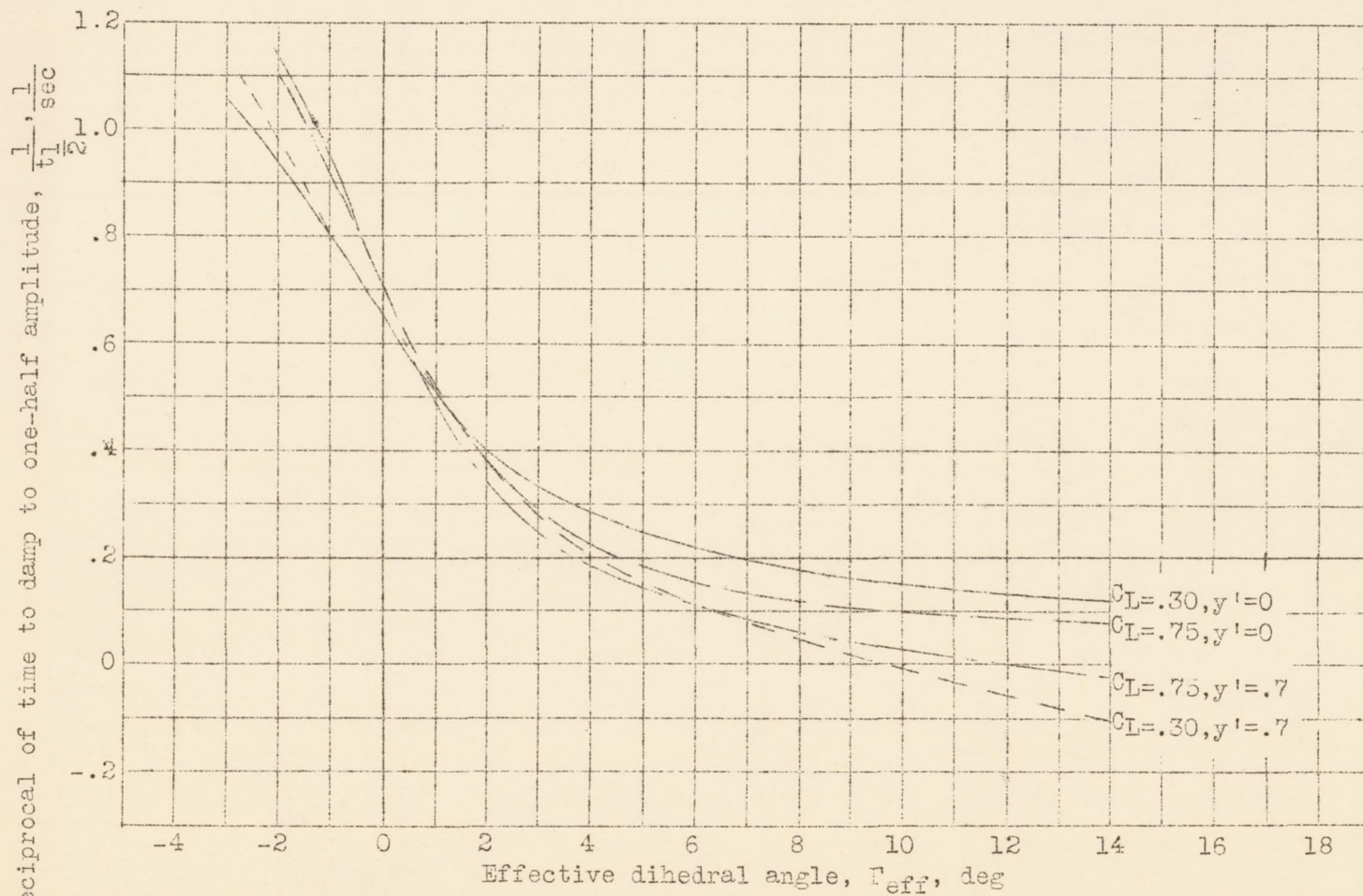


Figure 15.- Effect of lift coefficient on the damping of the aperiodic mode  $\lambda_2$  of a glider towed by a dyadic towline system.  $y'$  - span towlines.



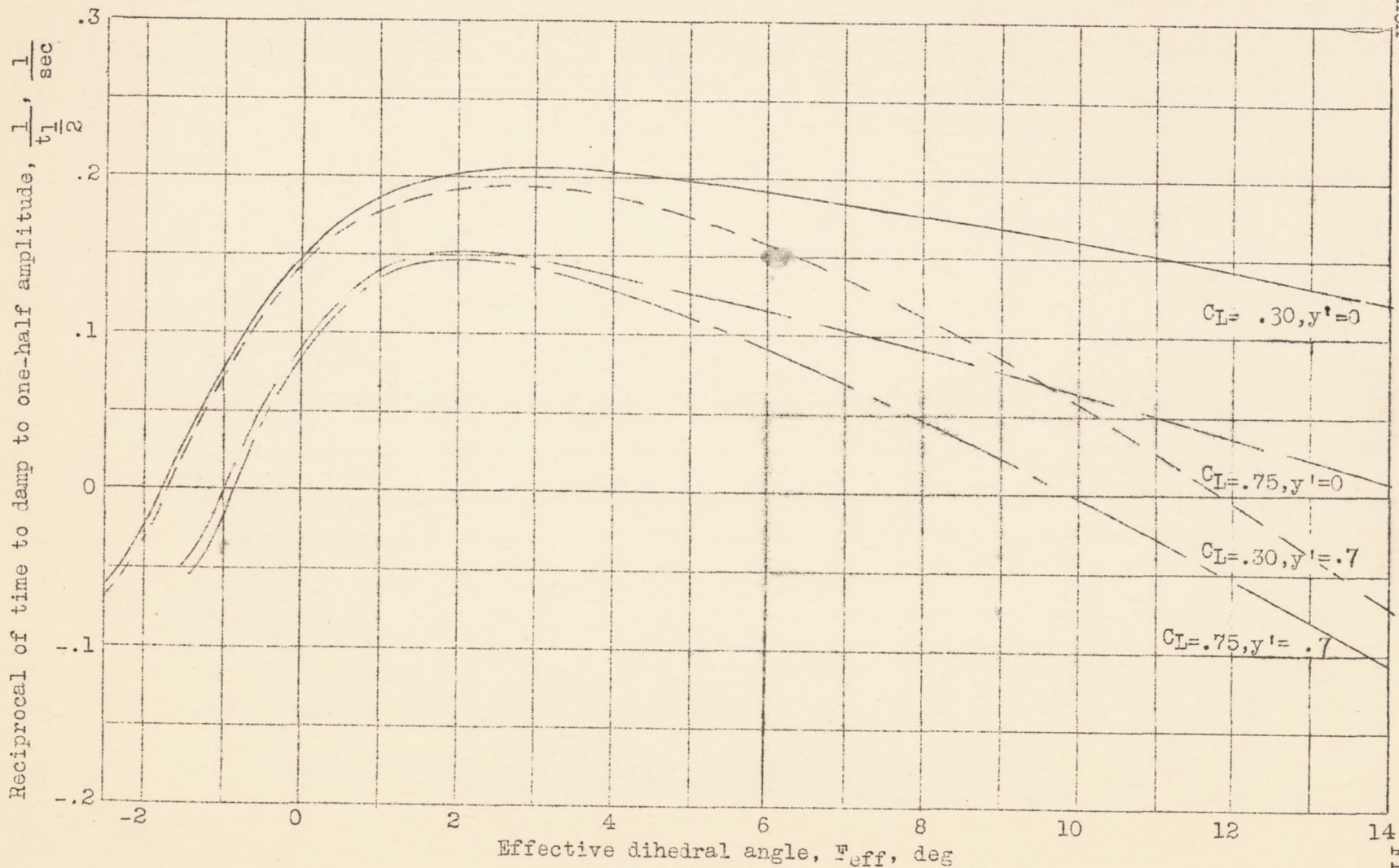


Figure 16.- Effect of lift coefficient on the damping of the periodic modes  $\lambda_3, \lambda_4$  of a glider towed by a dyadic tow system. 20-span towlines.

1877



1877

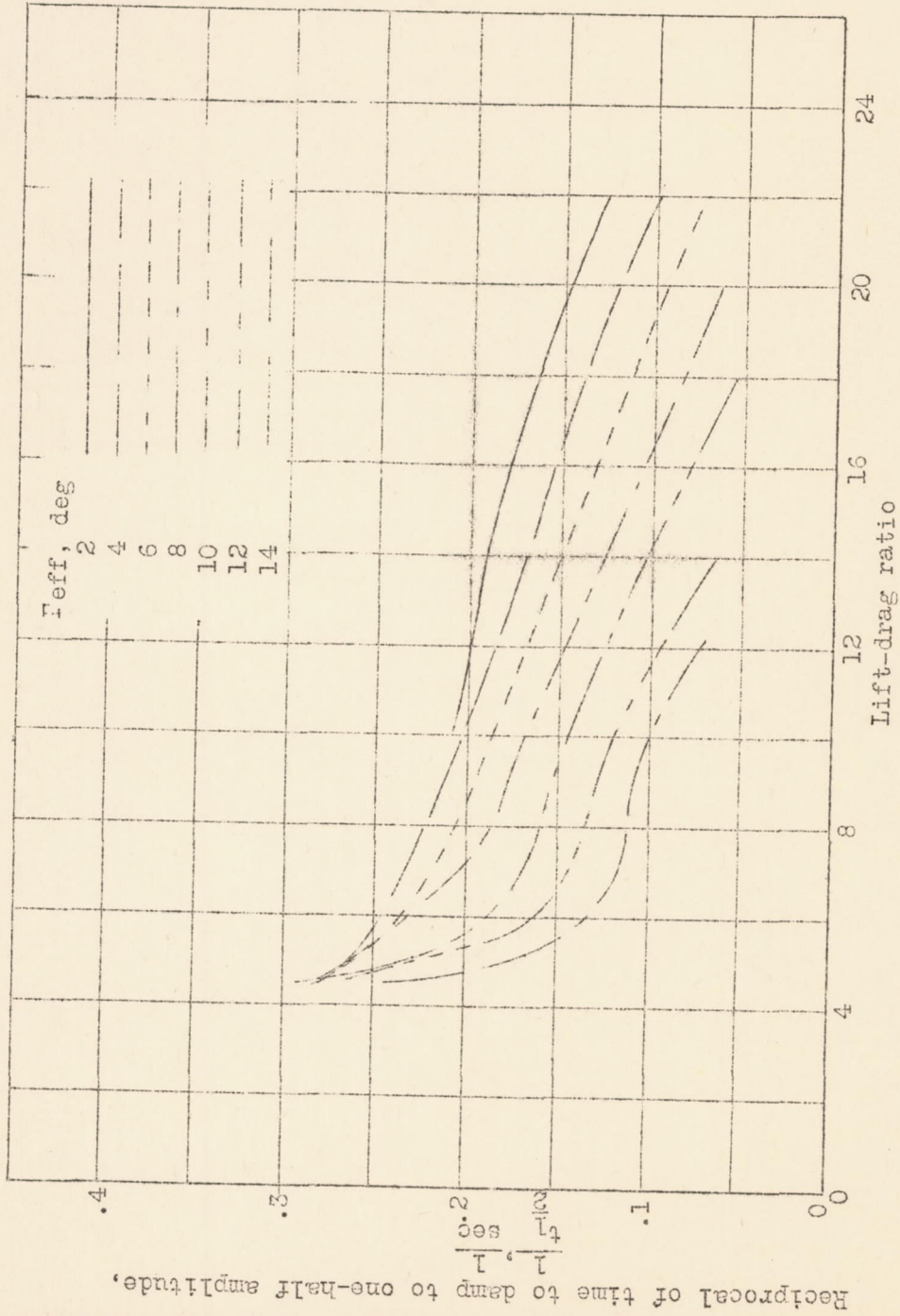


Figure 17.- Effect of lift-drag ratio on the damping of the periodic modes  $\lambda_3, \lambda_4$  of a glider towed by a dyadic tow system. 1 - span towlines  $y' = 0$ .